

1N-54  
375878

**NASA RESEARCH ANNOUNCEMENT  
FINAL REPORT FOR  
SPACE SUIT SURVIVABILITY ENHANCEMENT**

**September 25, 1998**

**Submitted By:**

Joanne S. Ware, John K. Lin and Thad H. Fredrickson  
ILC Dover, Inc.  
One Moonwalker Road  
Frederica, DE 19946  
<http://www.ilcdover.com>

Dr. Christopher M. Pastore  
Philadelphia College of Textiles and Science  
School House Lane & Henry Avenue  
Philadelphia, PA 19144-5497

**In Response To:**

NASA Research Announcement  
96-OLMSA-01B

**Contract Identification:**

NASW-97014

**Submitted To:**

Mr. Joseph Kroener, Code 210.H  
NASA Goddard Space Flight Center  
Greenbelt Road  
Greenbelt, MD 20771

cc:

Dr. Robert Norwood, NASA HQ  
Mr. Larry Chambers, NASA HQ  
NASA Center of Aerospace Information (2 copies)

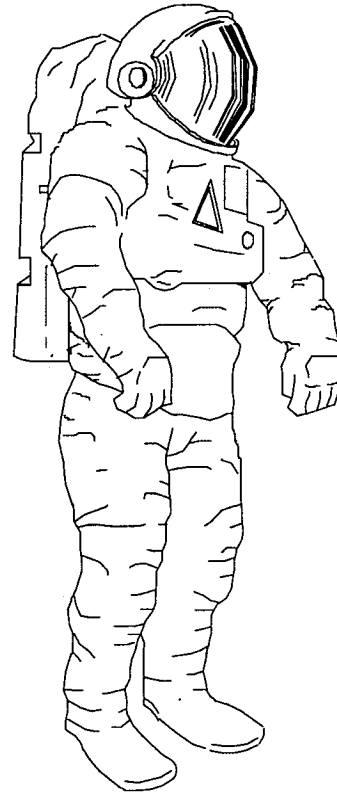


## TABLE OF CONTENTS

<u>Section</u>	<u>Title</u>	<u>Page</u>
1.0	<u>ABSTRACT</u> .....	1
2.0	<u>INTRODUCTION</u> .....	3
3.0	<u>BACKGROUND</u> .....	5
4.0	<u>APPROACH</u> .....	8
4.1	<u>SELF-SEALING MECHANISMS</u> .....	8
4.2	<u>CUT, PUNCTURE AND HYPERVELOCITY IMPACT RESISTANT MATERIALS</u> .....	10
5.0	<u>FINDINGS</u> .....	13
5.1	<u>SELF-SEALING MECHANISMS/MATERIALS</u> .....	13
5.1.1	<u>Background</u> .....	13
5.1.2	<u>Viscoelastic Material Candidates</u> .....	14
5.1.3	<u>Viscoelastic Fibrous Composite Material Candidates</u> .....	15
5.1.4	<u>Fibrous Composite Material Candidates</u> .....	17
5.1.5	<u>Self-Sealing Test Methods And Results</u> .....	18
5.1.6	<u>Self-Sealing Test Method</u> .....	18
5.1.7	<u>Self-Sealing Test Results And Discussion</u> .....	18
5.1.8	<u>Cold Flow Characteristic Test Method And Results</u> .....	22
5.1.9	<u>Recommendations</u> .....	22
5.2	<u>CUT, TEAR AND PUNCTURE RESISTANT MECHANISMS/MATERIALS</u> .....	22
5.2.1	<u>Puncture Mechanics</u> .....	23
5.2.2	<u>Tearing Mechanics</u> .....	25
5.2.3	<u>Cutting Mechanics</u> .....	27
5.2.4	<u>Fabric Design</u> .....	27
5.2.5	<u>Puncture Resistance Testing Method And Results</u> .....	28
5.2.6	<u>Cut Resistance Testing Method And Results</u> .....	29
5.2.7	<u>Cut And Puncture Recommendations</u> .....	30
5.3	<u>HYPERVELOCITY IMPACT</u> .....	30
5.3.1	<u>Background</u> .....	30
5.3.2	<u>Hypervelocity Testing Method And Results</u> .....	30
5.3.3	<u>Hypervelocity Impact Test Method</u> .....	32
5.3.4	<u>Hypervelocity Impact Test Results And Discussion</u> .....	32
5.3.5	<u>Recommendations</u> .....	33
6.0	<u>CONCLUSIONS</u> .....	34
7.0	<u>RECOMMENDATIONS</u> .....	35

## TABLE OF CONTENTS

### LIST OF FIGURES

<u>Figure</u>	<u>Title</u>	<u>Page</u>
1	Space Suit Materials Cross-Section .....	3
2	Self-Sealing Mechanisms Considered .....	9
3	Planform Of Samples .....	16
4	Cross-Section Of External And Internal Components.....	17
5	Cross-Section Of Assembled Samples .....	17
6	Self-Sealing Performance Comparison Chart .....	19
7	Self-Sealing Average Performance Comparison Chart.....	20
8	Schematic Of Fiber Mobility Subject To Small Penetrator .....	23
9	Schematic Illustration Of Successive Fiber Failure From Small Penetrator .....	24
10	Schematic Illustration Of Tear Resistance For Varying Degrees Of Yarn Mobility .....	26

### LIST OF TABLES

<u>Table</u>	<u>Title</u>	<u>Page</u>
1	SSA Vulnerability Summary .....	6
2	Self-Sealing Mechanisms Considered For Incorporation Into The SSA .....	8
3	Comparison Of The Selected Yarn Materials Physical Properties.....	12
4	Self-Sealing Material Trade Study.....	21
5	Cold Flow Characteristics.....	22
6	Overall Fabric Construction Parameters .....	28
7	Puncture Resistance Testing Results .....	28
8	Cut Resistance Testing Results .....	30

## **LIST OF APPENDICES**

APPENDIX A	SELF-SEALING CONCEPTS SUBMITTED FOR EVALUATION
APPENDIX B	LABORATORY ANALYSIS REPORT, SELF-SEALING PERFORMANCE TESTS
APPENDIX C	LABORATORY ANALYSIS REPORT, CUT PROTECTION PERFORMANCE TESTS
APPENDIX D	LABORATORY ANALYSIS REPORT, PUNCTURE RESISTANCE TESTS
APPENDIX E	HYPERVELOCITY IMPACT RESISTANCE TEST REPORTS

## REFERENCES

- ASTM F 1342-91 (Reapproved 1996) "Standard Test Method for Protective Clothing Material Resistance to Puncture", American Society of Testing and Materials.
- ASTM F 1790-97, (1997) "Standard Test Method for Measuring Cut Resistance of Materials Used in Protective Clothing", American Society of Testing and Materials.
- Cadogan, D., Kosmo, J. and Remington, B., "Enhanced Softgoods Structures for Space Suit Micrometeoroid/Debris Protective Systems," SAE Technical Paper No. 921258, July 1992.
- Christiansen, E.L., Lear, D., Prior, T., "Bomber EMU - Meteoroid/Orbital Debris Risk Calculations," NASA JSC Hypervelocity Impact Technology Facility, July, 1997.
- Gagliardi, D. D., and Gruntfest, I.J., "Journal of Textile Research", 20, p. 180, 1950.
- Gagliardi, D. D., and Nussele, A.C., "American Dyestuff Reporter", 39, p. 12, 1950.
- Hager, O.B., Gagliardi, D. D., and Walker, H.B., "Journal of the Textile Research", 17, 7, p. 376, July, 1947.
- Hodgson, E.W., Cupples, S., Cour-Palais, B.G., et al., "Micrometeoroid and Orbital Debris Hazard Considerations for Space Station-Related EVA," SAE Technical Paper No. 932225, July, 1993.
- Morton, W.E., and Hearle, J.W.S., Physical Properties of Textile Fibers, The Textile Institute, Manchester: 1993.
- Teixira, N., Platt, M., Hamberger, W., "Journal of Textile Research", 25, 10, 1955.
- Thomas, R.W., "Cut Resistance Testing of Industrial Gloves", Conference Proceedings: International Conference on Safety & Protective Fabrics, 1998.
- Tribble, Alan C., The Space Environment, Princeton University Press, Princeton, 1995.

## FINAL REPORT

### **SPACE SUIT SURVIVABILITY ENHANCEMENT NASW-97014**

#### **1.0 ABSTRACT**

Materials developed for the Extravehicular Activity (EVA) space suit have historically provided an effective barrier to the hazards encountered in space throughout the manned space program, with enhancements being made over time to accommodate changes in mission durations. As mission durations have changed, risks in the working environment have increased thus necessitating the need for evolutionary materials changes. Now, significant changes in mission durations are occurring again through the construction and habitation of the International Space Station and future Lunar/Mars missions. There is an anticipated three-fold increase in frequency of EVA work with the construction and habitation of the Space Station. The risks to the space suit that are anticipated from these endeavors include exposure to sharp objects that can cut or puncture, and penetrations from micrometeoroid/orbital debris (MMOD) impacts.

This research effort evaluated two broad-based methodologies that could increase the protection the space suit could provide. The first area of emphasis was to enhance the EVA suit's ability to avoid or withstand penetration of the Thermal Micrometeoroid Garment (TMG) and its underlying restraint and bladder, thereby preventing the loss of pressurization from the space suit. Self-sealing materials were developed to achieve this end. If incorporated into the space suit's cross-section (Figure 1) a self-sealing system of materials would repair penetrations to the pressure envelope, extending the current capabilities of the space suit. The second area of emphasis was the development of materials to resist cut and puncture threats, as well as benefit the space suit's MMOD impact protection capabilities.

The self-sealing mechanisms evaluated for their ability to increase the length of time before depressurization in the event that the space suit's protective layers are penetrated (which is currently 30 minutes with a 4 mm diameter hole (Christiansen et al, 1997) included: 1) viscoelastic materials, 2) nonwoven fibrous materials impregnated with viscoelastic materials, and 3) highly texturized fabric, adherent to the current bladder (pressure envelope) material. All candidates were bench tested in a pressurized state (4.3 psig) to assess their ability to seal a leak or puncture if used as the primary bladder material. The viscoelastic materials were the most promising of these candidates.

Cut and puncture resistant materials were designed from existing high tenacity/high performance yarns (Kevlar 29<sup>®</sup>) and newly developed high tenacity/high performance yarns (polyethylene naphthalate). Tested to measure their ability to prevent a breach in the pressure envelope, the most promising of these candidates were sent to the National Aeronautical and Space Agency

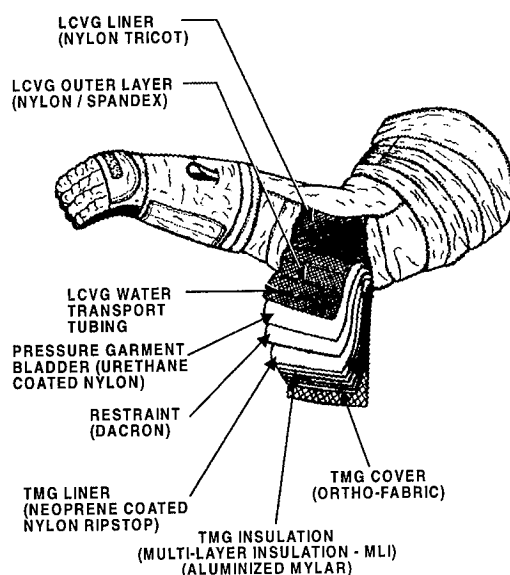
(NASA) Johnson Space Center (JSC) White Sands Testing Facility (WSTF)  
facility for hypervelocity testing.

## INTRODUCTION

The assembly and construction of the International Space Station will place unprecedented demands on the protection that the Space Suit Assembly (SSA) is required to provide. The harsh environment of space, and the increased frequency and scope of Extravehicular Activities (EVA), necessitate that increased space suit protection capabilities be addressed that have minimal to no increase in mass or flexibility. Through a joint effort, ILC Dover, Inc. and Philadelphia College of Textiles and Science addressed the enhancements the current space suit materials, with the following objectives: 1) to evaluate self-sealing or self-repairing mechanisms for the pressure envelope and 2) to evaluate newly designed fabric constructions for improving the protection capabilities of the space suit for resistance to cut, punctures, and Micrometeoroid/Orbital Debris (MMOD) impacts.

### *Space Suit Assembly Description*

The Extravehicular Mobility Unit, of which the SSA is a part, is a complete, self-contained life support system. This thermally controlled flexible structure provides the pressurized environment necessary for life sustaining functions. It facilitates required mobility and allows for tactility, while providing cut, puncture, and micrometeoroid protection. The SSA is constructed from many fabric layers to achieve these levels of protection. The space suit materials cross-section, Figure 1, identifies the different materials of the space suit that provide the required environmental, cut, puncture, air retention, and micrometeoroid protection.



**Space Suit Materials Cross-Section**

**Figure 1**

The two fabric layers of the SSA, the pressure envelope (bladder) and the Thermal Micrometeoroid Garment (TMG) Shell, chosen for enhancement research were done so for the critical role they play in the protection of the astronaut. These layers maintain pressurization and resist cuts, punctures, and MMOD impacts.

### *The Pressure Envelope*

The pressure envelope is currently a polyester polyurethane laminated nylon fabric. The envelope is a heat sealed construction and is inflated to 4.3 psia during EVA. The laminated envelope functions to maintain the pressurized environment within. At present, in the event that the system loses pressurization, it has no ability for self-repair. The current space suit design allows for a 30 minute window to return to the safety of the Space Shuttle or the Space Station should a breach no larger than 4 millimeters in diameter occurs in the pressure envelope.

### *Thermal Micrometeoroid Garment*

The TMG Shell is a multi-layered fabric, with the outermost layer composed of a woven double cloth construction. It consists of tetrafluoroethylene (Gortex<sup>®</sup>), meta-aramid (Nomex<sup>®</sup>), and para-aramid (Kevlar<sup>®</sup>). The outermost (exterior or fabric face) layer of this fabric is Gortex<sup>®</sup>, and is positioned for its characteristic solar reflectivity. The inner layer of this fabric (back) is of a ripstop construction, with Nomex<sup>®</sup> as the resilient, high strength primary component, and Kevlar<sup>®</sup> as the "rip-stop" yarns which provide additional puncture and tear resistance.

The middle layers of the TMG are composed of a scrim reinforced aluminized mylar which provides the majority of the thermal protection offered by the space suit. The layers are positioned such that the reflective surfaces face the exterior of the space suit, reflecting infrared radiation away from the body. The scrim reinforcement of each of the layers separates the reflective aluminized surfaces, thereby minimizing heat conduction between layers. These layers and intervening spaces provide not only thermal protection to the space suit, but assist in absorbing ballistic energy. The last layer, or inner most layer, of the TMG is a neoprene coated woven nylon fabric which specifically functions for MMOD impact absorption. Current hypervelocity impact test data supports the hypothesis that a multi-layered construction provides enhanced protection over that found in an equivalent single layer of material.

### 3.0

## BACKGROUND

The solar system contains naturally occurring "debris" called micrometeoroids (MM) which result from the breakup and collision of comets, asteroids, etc. Man has been contributing to this "debris" since the inception of space programs. The artificial debris generated from space programs originates from nonoperational spacecraft, boosting stages, solid rocket fuel particles, etc. and is referred to as orbital debris (OD). However, the portion of the spectrum that was addressed in this effort were the majority of MMOD which are less than 1 cm in size. These present a significant threat to EVA due to the large kinetic energies associated with impacts at orbital velocities. The following represents kinetic energy. Resulting impacts can then be inferred.

$$KE = 1/2mv^2$$

Since orbital impacts occur at speeds on the order of 10 km/s and assuming a density of 1 g/cm<sup>3</sup>, particulate matter impacting at this speed will carry significant kinetic energy. Particles as small as 0.1 mm may cause surface erosion on impact, while a 1 mm size particle would pose a significant threat and would inflict serious damage upon impact.

Hypervelocity impact characteristics are a function of velocity at impact. When impacting speeds are less than 2 km/s, the projectile will remain intact. When impacting speeds are between 2 and 7 km/s, the particle will shatter into fragments. At speeds between 7 and 11 km/s on impact, the particle will transform into molten state, and at speeds above 11 km/s, the particle may vaporize. Of course, the state of the particle upon impact will affect the physical processes responsible for transferring kinetic energy to the target. Kinetic energy will also cause incidental destruction upon impact through the creation of holes or craters into the target. If the hole is large enough, the surface may be penetrated. (Tribble, 1995) If this scenario occurs, it will allow the impacting material to damage the outer layer of the TMG and the fabric layers lying beneath it. Any compromise to the integrity of the TMG can potentially compromise the pressure envelope and the safe environment which it provides.

### *The Micrometeoroid and Orbital Debris Environments*

Examinations of surfaces and data from the Long Duration Exposure Facility (LDEF) after exposure to hypervelocity impacts in space have allowed models to be developed for size and frequency distributions of naturally occurring MMs. Observations via radar indicate that there is a slight variation of flux over the course of the a year. This variation occurs when the Earth's orbit intersects the orbital path of the cloud of dust left by the break-up of a comet, or micrometeoroid shower. Where the average MM velocity is 17 km/s, the average OD velocity is 8 km/s. Unlike the MM, the OD flux is affected by the solar cycle (via aerodynamic drag). When comparing the flux of equal size particles, the OD environment in some of the more populous orbits currently exceeds the MM environment. It is estimated that there may be as many as 20,000 pieces of

debris greater than 4 cm currently circling the Earth and it is not unexpected that particulate material ejected from hypervelocity impacts may go on to become orbital debris itself. Though considered to be a certainty in space flight, the probability of impact with another object is estimated from the following relationship, where in time T (years) the number of impacts an object of surface area A(m<sup>2</sup>) can expect is given by:

$$N = \int_t^{t+T} FA dt$$

while the probability of n impacts is given by

$$P_n = \frac{N^n \exp^{-N}}{n!}$$

Hodgson, et. al provided an SSA Vulnerability Summary (Table 1) by linking SSA material surface areas to their respective area densities, and then estimating the resulting protective capabilities of those regions to MMOD through correlations for penetration of monolithic layers of materials. It is important to note that these estimates are expressed in terms of the critical particle size for MMOD which will just penetrate the TMG in each of these regions. These critical particle sizes are combined with the size distributions for each of the regions to estimate the total probability of penetration of the SSA.

**Table 1**  
**SSA Vulnerability Summary**

Description	Area (m <sup>2</sup> )	Areal Density (g/cm <sup>2</sup> )	Debris (cm)	Penetration Threshold	
				Micrometeoroids (cm)	Hazard (%)
Lower Torso	1.2	.13	.032	.035	50
Arms	.75	.13	.032	.035	29
Gloves	.11	.07	.02	.02	15
PLSS	.9	.94	.13	.13	2
DCM	.18	.51	.062	.065	2
HUT	.12	.44	.064	.07	1.2
Helmet (Visor)	.06	.37	.063	.07	.6
Helmet	.15	.61	.14	.15	.2
Boots (Soles)	.05	1.5	.26	.27	<.1

As Table 1 indicates, the greatest percentages of exposure to MMOD threats are found in the Arms, Lower Torso, and Gloves. This research effort concentrated on improving materials for the outer layer of the TMG that would be found in all of these areas, and self-sealing capabilities in all but the gloves.

Sharp object exposure that poses potential threats such as cuts and punctures to the SSA will also occur during the construction and habitation of the International Space Station. The astronaut has intended as well as unintended contact with sharp, unprotected, or damaged edges of spacecraft or component parts, which presents a significant threat to the protection that the space suit can offer. The design of the SSA must account for the sorts of complex situations that arise where hand-holds or contact surfaces are confronted while on an EVA mission. Two examples describe the sort of threats that the SSA has faced in the past: 1) During the EVA on STS-72 in which practice techniques for the assembly of the space station were conducted, significant damage to the space suit, in the form of cuts in the TMG of the gloves surface, were noted. These cuts were attributed to the hardware being used to carry out the missions (Fritz, 1996). This damage was created by sharp edges from a tool cabinet and a translation cable. In this instance the damage did not reach the pressure envelope, this structural integrity was maintained. Though there are specifications for surface edge geometries for the Shuttle program, they are not always followed, and not all contacts with risk can be averted. 2) Another, more extreme example of the dangers that advanced EVA holds, occurred during STS-49 when the Intelsat VI was captured. The astronauts and ground crew averted potential disaster involving cuts or penetration of the pressure envelope. During this mission there was significant concern generated regarding a possible SSA penetration when the 0.062 inch thick metallic surface of the satellite was grasped by three EVA astronauts. Fortunately, the spinning satellite's inertia was low enough not to require the gloves or any other part of the SSA to be dragged along the potential knife edge. As stated earlier, the TMG offers a critical role in protecting the astronaut. The need for improving the safety factor of the TMG and the pressure envelope is becoming especially acute as orbital repair and construction activities become routine.

#### 4.0 APPROACH

By concentrating research efforts toward the three primary areas of focus, 1) self-sealing capabilities for the pressure envelope, 2) improved cut and puncture, and 3) hypervelocity impact resistance for the TMG, significant accomplishments were met, encouraging continued investigation and development in these areas.

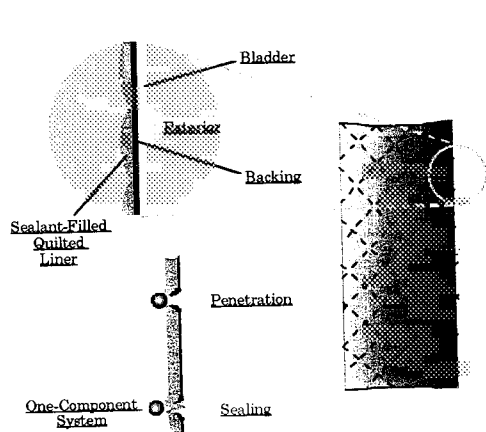
Unshadowed areas of the torso and extremities, where exposure to MMOD is highest, were felt to be an important focus for these enhancement efforts. Therefore, TMG enhancement technologies were directed only to unshadowed areas of the TMG with the glove as an exception. The glove, though extremely critical, has unique requirements for mobility and tactility. Design changes, no matter how slight, have a much greater affect on functionality than a similar change to another area of the space suit. It was decided that developmental enhancement efforts for the glove would be better served from a stand-alone effort, and not combined with developmental efforts for the remainder of the TMG and pressure-envelope.

#### 4.1 SELF-SEALING MECHANISMS

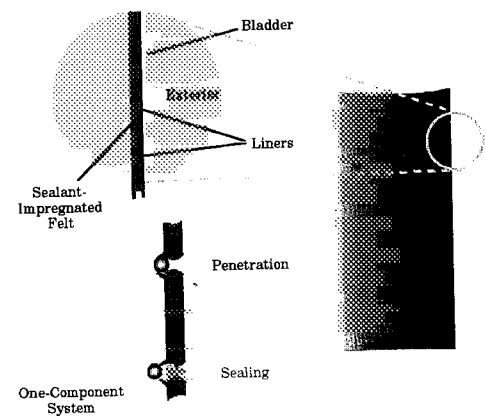
Various concepts for potential self-sealing mechanisms were evaluated (Table 2) with the anticipated goal of a self-sealing pressure envelope that would be characteristically soft and easily distorted upon the application of compressive, tensile, or shear force(s). It was also desired that the selected medium would possess the ability to return to an original shape once external force(s) were removed. Successful research efforts led to a separate layering of viscoelastic materials as the most desirable of all methods evaluated.

**Table 2**  
**Self-Sealing Mechanisms Considered For Incorporation Into The SSA**  
**(Reference Figure 2)**

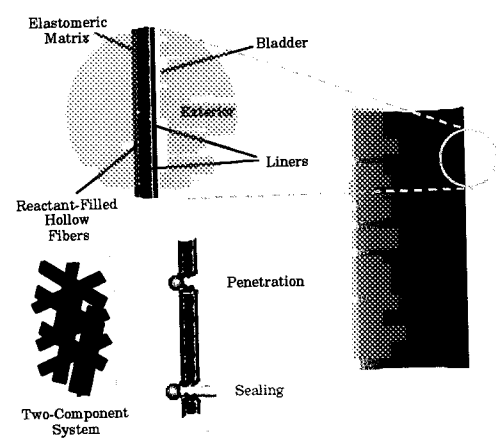
Conceptual Approach	Sealing Mechanism	Rationale
<b>Liquid Sealant Concepts</b>	Quilted Sealant	• Quilted liner incorporating sealant located adjacent to the pressure envelope.
	Impregnated Felt	• Fibrous material composite maintaining sealant stable located adjacent to pressure envelope.
	Viscoelastic Layering	• Separate self-sealing layer located adjacent to the pressure envelope.
<b>Foaming Concepts</b>	Filled Fibers	• A layer of hollow fibers filled with foaming reagents that mix and react to seal when ruptured.
	Embedded Capsules	• Micro-embedded foaming reagents are embedded in an elastomer mix and react to seal when ruptured.
<b>Mechanical Sealant</b>	Blousy Fabric	• Oversized blousy fabric positioned beneath the bladder is pulled through the fabric puncture by air flow upon rupture.
<b>Environmental Response</b>	Reactant Layer	• Low viscosity elastomer rapidly increases in viscosity when exposed to moisture.



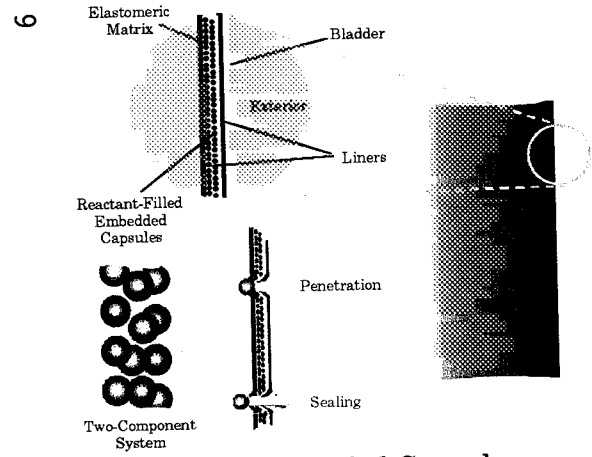
Quilted Sealant



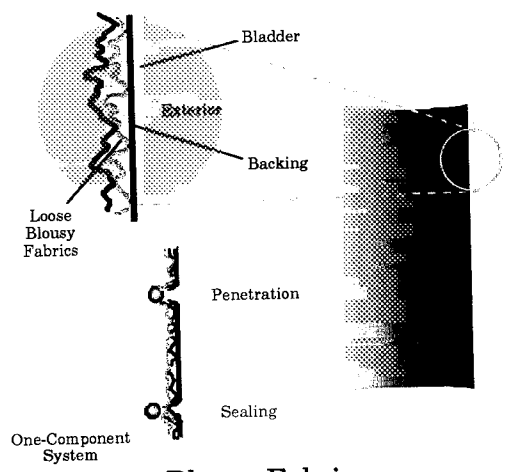
Impregnated Felt



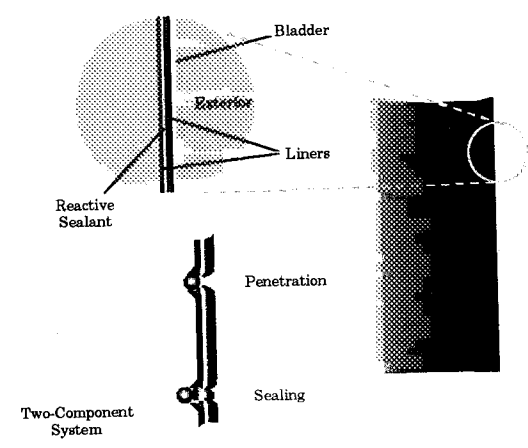
Filled Fibers



Embedded Capsules



Blousy Fabric



Reactant Layer

Self-Sealing Mechanisms Considered for Incorporating into the SSA  
Figure 2

Viscoelastic Materials - These materials combine both viscous and elastic behaviors, which means that they both dissipate and store energies. Elastomers (i.e. rubbers) are the best known examples of this class of material. The material is made from long, flexible chain-like molecules. They contain many single valence bonds, about which rapid rotation is possible as a result of thermal agitation. Thousands of these molecules are linked together into a chain to form an elastomeric unit. Such molecules will change shape readily and continuously at normal temperatures by Brownian motion. They take up random conformations in a stress-free state, but assume somewhat oriented conformations if tensile forces are applied at their ends. In other words, any deformation will tend to "straighten out", or uncoil, the entangled mass of contorted chains, and these will tend to coil up again when the restraining force is released. This elastic-retractile force is really due to the violent contortions of the long, flexible chains. By incorporating a small number of intermolecular chemical bonds (i.e. crosslinks) into the elastomer, a permanent structure with the optimal crosslinking density can be formed. Silicone and urethane polymers are two types of viscoelastic materials having exceptional behavioral responses for this sort of function (Cadogan, 1996).

Silicone Polymers - Silicone Polymers (polydimethylsiloxane), available in a variety of molecular weights and with varying degrees of cross-linking can form a variety of desirable compounds. They have low and predictable tensile and compressive moduli. With good cohesive strengths they tend to adhere well to themselves in a low crosslinked state. Silicone polymers are chemically inert and possess an excellent combination of low temperature flexibility and high temperature resistance.

Urethane Polymers - Urethane Polymers can also be tailored to desired performance requirements. Derived from the reaction of diisocyanate and diol, urethanes possess high strength, high elongation, and have a predictable moduli. Varying the ratio of starting materials, urethane polymers can range from a soft pliable gum consistency to a rigid, hard polymer.

## 4.2 **CUT, PUNCTURE, AND HYPERVELOCITY IMPACT RESISTANT MATERIALS**

Materials that were soft, flexible, and resilient were developed for the cut and puncture resistance effort. Though the fabric currently used as the outermost layer of the TMG is a double-cloth construction, for this effort, these single layer fabrics allow for significant alterations in fabric construction (layers, basic weave design, yarn inlays) as would be deemed necessary from testing results. High molecular - high tenacity (HM-HT) materials such as those chosen for this effort, were done so as they possess a degree of crystallinity (the orderly or parallel arrangement of polymer molecules within and along a fibers axis) and of orientation (the degree to which linear polymeric chains are parallel and oriented in a preferred direction, which may not be that of the fiber's axis) which are important determinants to cut and puncture resistance that these materials

can provide. The high tenacity, high performance yarns utilized in the prototypes were para-aramids (Kevlar 29<sup>®</sup>) and polyethylene naphthalate (PENTEX).

### Para-aramid Fibers

Para-aramid fibers are composed of the aromatic polyamide, poly (p-phenylene terephthalamide) or PPTA:



These molecules are stiff and possess strong tendencies for interaction with neighboring molecules, both at the benzene rings and by hydrogen bonding at the -CO.NH- groups. In solution these self-attracting molecules form elongated liquid crystals. High shearing at this point of fiber formation aligns the crystals, parallel to the fiber axis, resulting in a fibrous structure that consists of fully extended chains, packed together with a very high degree of crystallinity and orientation. A slight disorder is present which originates from boundaries between liquid crystals and imperfections of packing within the crystals resulting in some departure from perfect orientation. When drawn, (the act of applying tension, either during extrusion or immediately thereafter), these fibers improve their structural perfection. Kevlar 29<sup>®</sup>, used in both the current TMG and the newly developed prototypes, is a lower-ordered, lower-modules form of the para-aramids. Within the crystalline lattice formation there is an alternating ring and linear formation which creates an anisotropic situation. Though highly crystalline and oriented, this creates a radically oriented axial pleating of the crystalline sheets, which helps to resist to some degree, compressive forces while maintaining high strength characteristics.

### Meta-aramid Fibers

Meta-aramid fibers (Nomex<sup>®</sup>) are made from poly (*m*-phenylene isophthalamide). By comparing to the para-aramids, the shape of these molecules prevent liquid-crystal formation which results in a partially oriented, partially crystalline structure. For this reason Nomex<sup>®</sup> possesses higher elongation properties than does Kevlar<sup>®</sup>, and possesses a lower tenacity.

### Polyethylene Naphthalate Fibers

Structurally, the polyethylene naphthalate fibers (PENTEX) are more similar to the para-aramids than to the meta-aramids. They possess a significantly higher compressive modulus compared to the other materials, which would prove beneficial to resisting cut and puncture threats.

**Table 3**  
**Comparison Of The Selected Yarn Materials Physical Properties**

	<i>Kevlar 29</i>	<i>Nomex</i>	<i>PEN</i>
Density (g/cc)	1.44	1.38	1.39
Tenacity (g/d)	23	4 - 5.3	10+
Modulus (g/d)	550	550	250
Elongation (%)	4.0	22-32	6.0
Compressive Modulus (g/d)	.39	.39	3.6

## **5.0 FINDINGS**

As purported, the goal of this study was to define and test materials that could offer improved performance in the areas of self-sealing, cut and puncture resistance and improved protection against hypervelocity impacts. These three areas are discussed in detail in Sections 5.1, 5.3 and 5.5 respectively.

### **5.1 SELF-SEALING MECHANISMS/MATERIALS**

ILC Dover collaborated with the Philadelphia College of Textiles and Science in the design of these self sealing materials and mechanisms. As shown in Table 2.0, several approaches were considered. Some of the more exotic concepts (i.e. microencapsulation as one example), although interesting from a technology viewpoint, were not pursued because they were clearly beyond the original scope of the proposal. It was decided that we would concentrate on both liquid sealing concepts as well as a mechanical sealing concept as proposed by Philadelphia College of Textiles and Science.

#### **5.1.1 Background**

As discussed in Section 4.0 of this report, viscoelastic materials exhibit the fundamental properties for self sealing behavior. Since they exhibit both viscous and elastic properties, they do possess sufficient memory to return to their original location after being punctured or torn. In addition, it is also important that a polymer system possess high affinity for itself after being damaged. This strong attraction, along with its a high cohesive strength, ensures that the damaged material can "mend" itself in a reliable manner.

It was anticipated that the ideal candidate would be relatively soft and easily distorted upon application of a compressive , tensile or shear force. Once the force is removed, the elastomer should return to its original shape. If the elastomer layer is breached, it would readily flow upon itself and knit together in a strong, cohesive bond. The data presented in section 5.1.8 supports this theory.

Practically speaking, some type of permanent structure is necessary to form a coherent solid and prevent liquid like flow of elastomer molecules. This requirement is usually met by incorporating a small number of intermolecular chemical bonds (i.e. crosslinks) to make a loose three dimensional molecular network. These crosslinks further affect the elastic behavior of the molecule. Through proper selection of the elastomer and crosslink density, the desired properties can be obtained.

Two types of polymer systems were investigated and tested in this study. Silicone polymers, based upon polydimethylsiloxane, are available in a variety of molecular weights and can be crosslinked to form a variety of compounds. They exhibit low permanent set properties and tend to adhere well to themselves in a low crosslinked state. Secondly, urethane polymers are another class of

elastomers that can be tailored to meet the desired performance requirements. By varying the mole ratio of the starting materials, urethane polymers can be produced ranging from soft, pliable gums to rigid, hard polymers.

### 5.1.2 Viscoelastic Material Candidates

Listed below is a description of the silicone and urethane candidates investigated in this study. In all cases, the materials submitted for puncture testing were laminated to a lightweight, 220 denier polyester basecloth to facilitate handling and to increase its overall damage tolerance.

#### *Silicones*

**Silastic HS-30**, produced by Dow Corning Corporation, is a 30 Shore A durometer, high strength methyl-vinyl silicone elastomer. It is compounded with 2,4-dichlorobenzoyl peroxide catalyst and put into solution with toluene. The silicone rubber solution is then coated onto the lightweight polyester cloth at the desired thickness and vulcanized in a hot air oven. This candidate exhibited poor self sealing behavior in early testing and was therefore dropped from further consideration.

**SWS 7810**, manufactured by SWS Silicones, is a 10 Shore A durometer, methyl vinyl silicone elastomer. As with the Silastic HS-30, it is compounded with a suitable peroxide catalyst and coated onto a fabric. The goal here was to evaluate a softer version of this type of elastomer for improved self sealing properties. Unfortunately, this softer material exhibited poor results in early testing and was dropped from further consideration.

**Sylgard Q3-6636**, manufactured by Dow Corning Corporation, is two part, dielectric silicone gel designed for potting and encapsulating moisture sensitive electronic circuitry. It is reported to retain the stress relief of a liquid while developing the dimensional stability and nonflow characteristics of an elastomer. In fact, it is reported to possess self healing properties as well as pressure sensitive adhesive bonding properties. Its hardness is well below that of conventional silicone gum rubbers (as described above). In fact, hardness is typically expressed in terms of penetration of a probe for these soft gels.

#### *Urethanes*

**Rucothane CO-AX-5294**, manufactured by Ruco Polymer, is a urethane solution polymer based upon thermoplastic, polyether urethane. It is presently used in the manufacture of all glove bladders for the current Shuttle Space Suit contract. It possesses high tensile and tear strength in combination with a relatively low tensile modulus. It is included here since it has demonstrated some self sealing abilities during EVA where the astronauts palm bar penetrated the glove bladder. The bladder was able to form a seal around the metallic palm bar and the leakage was stopped.

**Conathane EN-11**, manufactured by Conap Incorporated, is a two part urethane used for potting and casting applications. It exhibits lower hardness and modulus than the Rucothane polymer, and therefore would be expected to perform better in a self sealing application.

**TyrLyner**, manufactured by Synair Corporation, is a two part urethane used for self sealing passenger car tire applications. In its cured state, it behaves like a soft gel, with very low hardness and low modulus properties. In many respects, it is analogous to the silicone gels in the silicone family of polymers. Part A is described as the curative consisting of a hydroxyl terminated polyether polyol. Part B is defined as a isocyanate terminated prepolymer.

As described in section 5.1.7, selected materials have been tested in 15 and 30 mil thicknesses. In all cases, the material has been laminated to a 220 denier, high count polyester fabric to increase its durability.

### **5.1.3 Viscoelastic/Fibrous Composite Materials**

The self sealing material candidates used in combination with textile reinforcements to form a flexible composite construction are described in Table 2. All of the self sealing test coupons were prepared per the following procedure:

The current bladder cloth (polyester polyurethane laminated nylon fabric) was cut into six-inch diameter circles, one for each sample prepared. The coated side of all of the bladder cloth circles was swabbed with acetone to remove any parting film. Cloth discoloration was not observed nor were any coloration nor deposits observed on the swab.

All of the samples had the configuration shown in Figure 3.

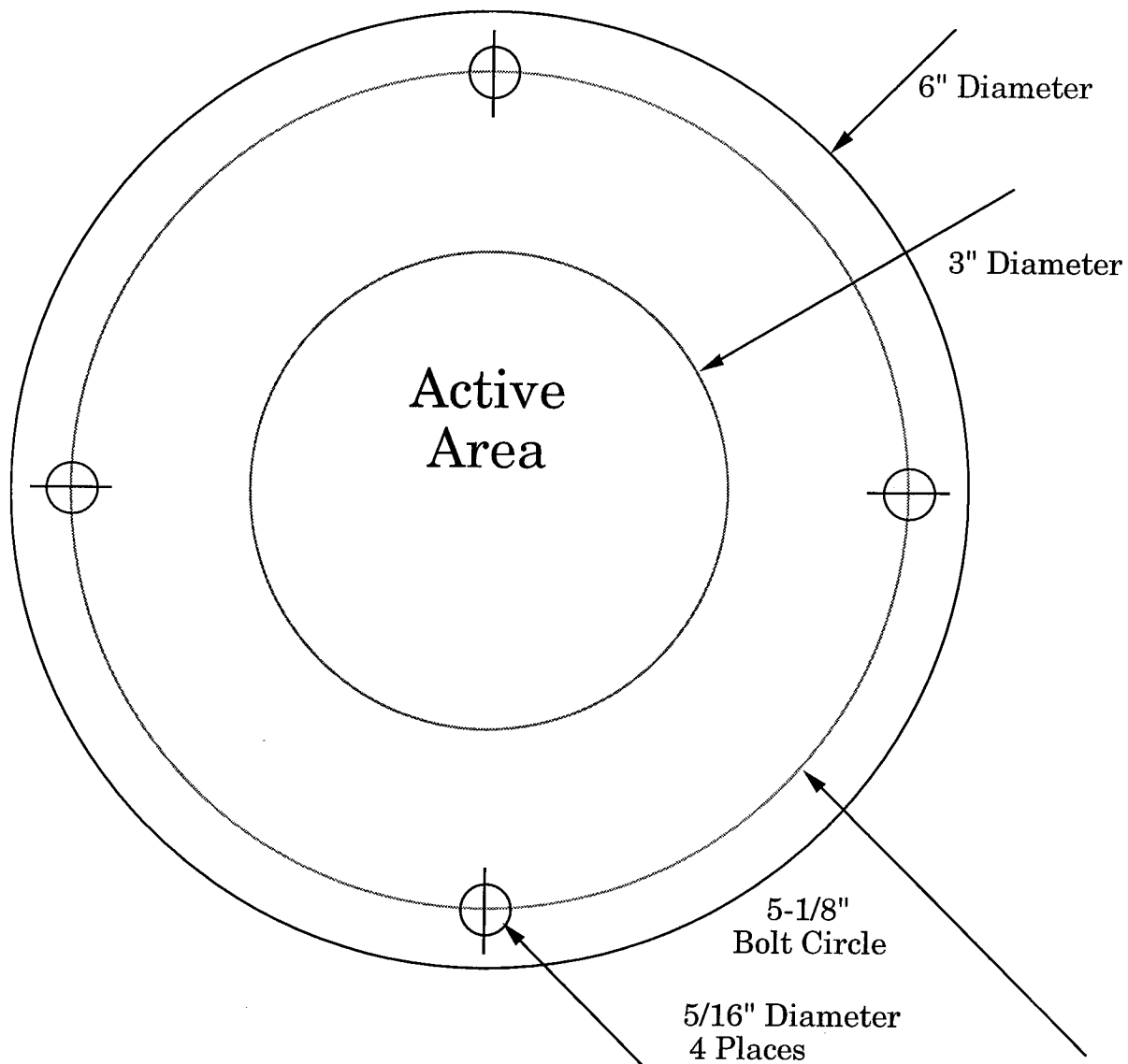


**Figure 3. Planform Of Samples**

The filled-felt samples were prepared from six-inch diameter circles cut from a generic felt blanket with an adhesive siding, two felt circles for each sample. The particular commercial felt used for these samples was Model #32034 distributed by Faultless Caster of Evansville. The four filler compounds employed were:

- Silicone Vacuum Grease purchased by Dow Corning**
- Tyrllyner Isocynate as described in Section 5.1.2**
- Conathane as described in Section 5.1.2**
- Wacker Sigel is a silicone elastomer supplied by Wacker**

These compounds were prepared according to manufacturer's directions. The compounds were manually infiltrated the filler material into the felt using a spatula. As shown in Figure 4 the samples were prepared as two separate components.

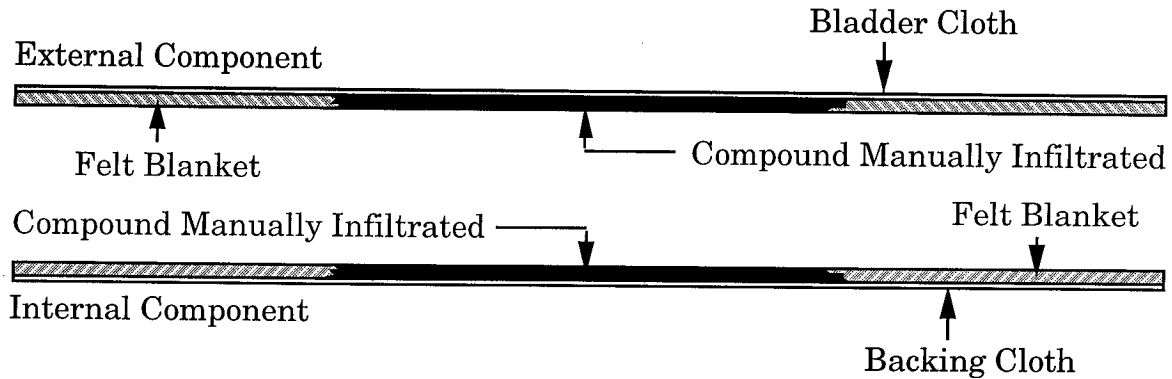


**Figure 4. Cross-Section Of External And Internal Components**

The samples were assembled from the external and internal by pressing together and the components secured by a circumferential line of stitches as shown in Figure 5.

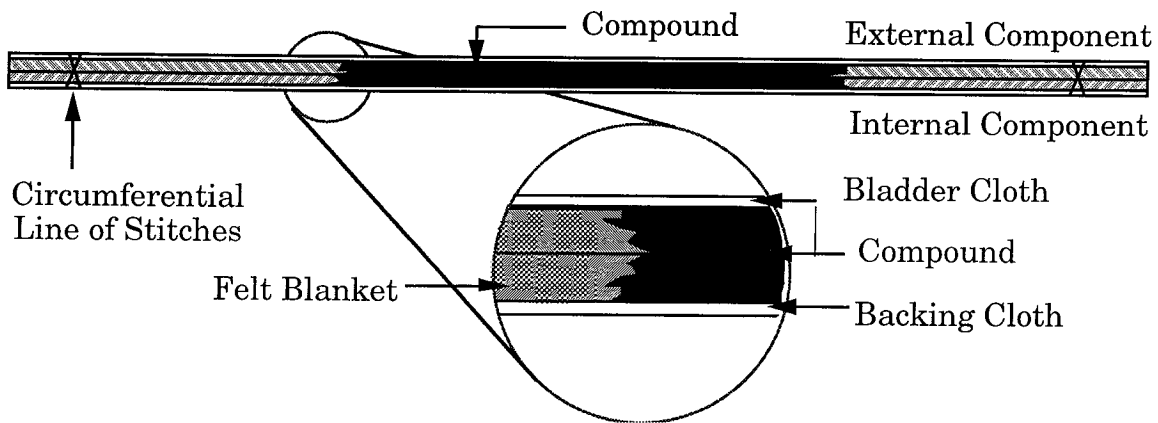


**Figure 5. Cross-Section Of Assembled Samples**

The samples were roughly 0.15 inches thick after assembly.

#### 5.1.4 Fibrous Composite Materials

This concept is described under the heading “mechanical sealant” in Table 2. The idea is to have a very fine “blousy” fabric pulled through the fabric by the internal air pressure upon puncture of the bladder.

The blousy samples were fabricated from a polyolefin crepe cut into 2.5 inch diameter circles. Epoxy cement spots were placed in a square pattern on the crepe and the crepe cemented to the bladder cloth, bellowed between the spots. Two layers of crepe were used for each sample.

#### **5.1.5 Self-Sealing Testing Methods And Results**

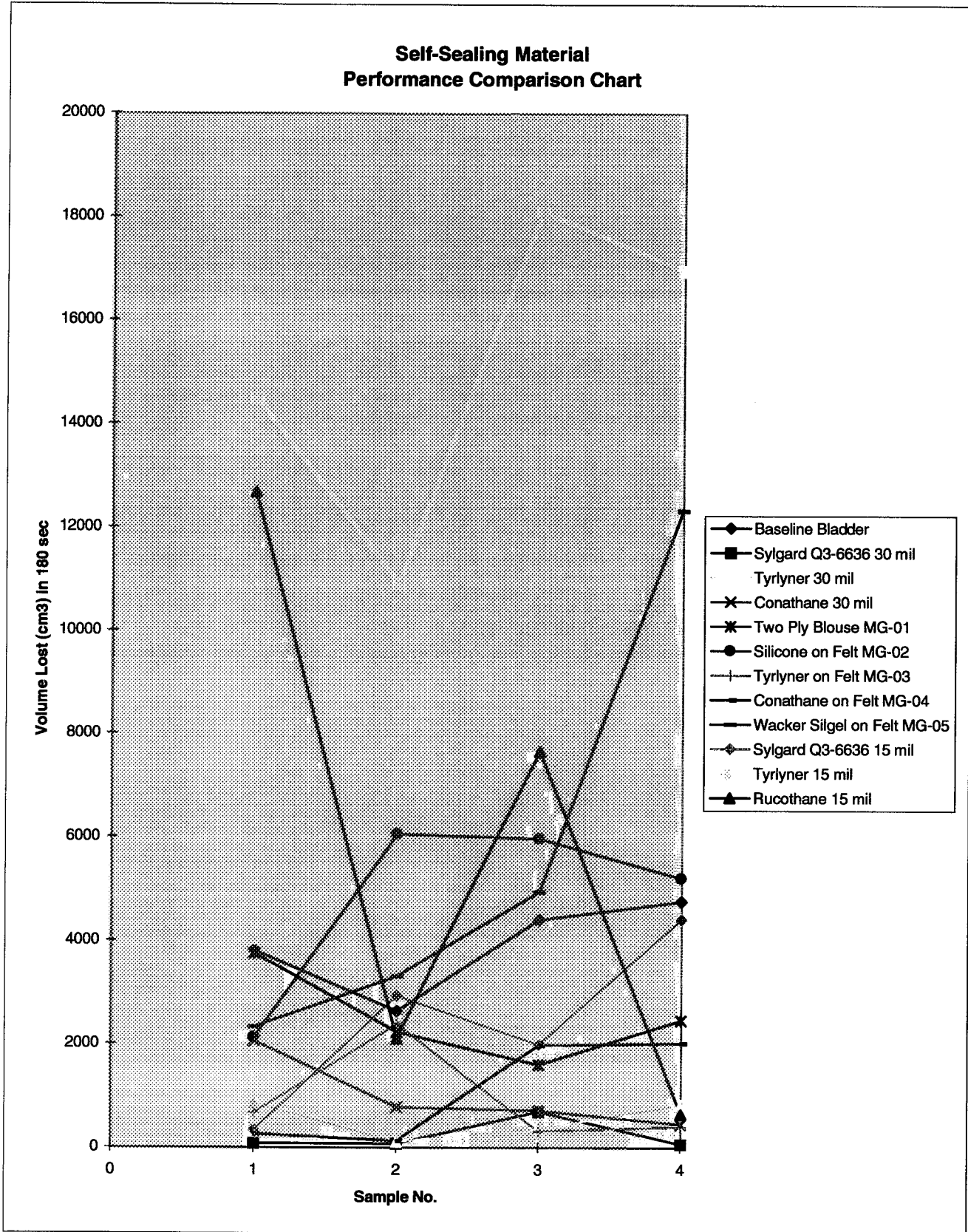
#### **5.1.6 Self-Sealing Test Method**

ILC Dover developed the "Standard Test Method for Measuring Self-Sealing Characteristics of Materials Used In Inflatable/Pressurized Protective Clothing" (ILC Document No. 1275-70001) to evaluate self-sealing characteristics of a self-sealing material specimen by measuring the time required to effectively seal the pressurized test fixture after a puncture probe (meeting the testing probe requirements of ASTM F1342-91, with a 2.0 mm diameter of a length of 3.2 mm) had compromised the specimen causing leakage. Before testing, sample specimens were prepared according to the design specification detailed in the test method. Each sample specimen was identified and its physical and chemical properties recorded. Those materials with special shelf life and storage requirements were also noted.

#### **5.1.7 Self-Sealing Test Results And Discussion**

Data for the self-sealing materials were gathered from twelve different samples including the current space suit bladder as a baseline control. Five data points were collected per second, for pressure, gas flow rate, and force of penetration. In addition, strike plate contact was used to confirm penetration. Each set of tests were analyzed for self-sealing characteristics by looking at the volume lost over 3 minutes (volume lost is calculated by applying Simpson's rule using rectangular left-hand endpoint approximation), minimum pressure after puncture, maximum flow rate after puncture, minimum flow rate after puncture, and the time required for the flow rate to reduce from maximum to minimum.

All the samples tested exhibited self-sealing characteristics. They all had a logarithmic decaying function. However, not all the samples tested performed better than the baseline bladder. From the analysis reports (Appendix C) and the performance summary charts included in the text, we can see that the Sylgard Q3-6636 performed consistently better than the baseline whether constructed as a separate layer or impregnated into felt. Single layer 30 mil thick Sylgard Q3-6636 performed best. The average gas volume lost over 3 minutes after puncture is 227.25 cm<sup>3</sup>. Another trend observed from this analysis is that the single layer 30 mil thick specimens performed consistently better than those with felt. However, when the thickness of the single layer construction is reduced from 30 to 15 mils, performance was reduced to below those with felt, the Sylgard Q3-6636 being the exception.



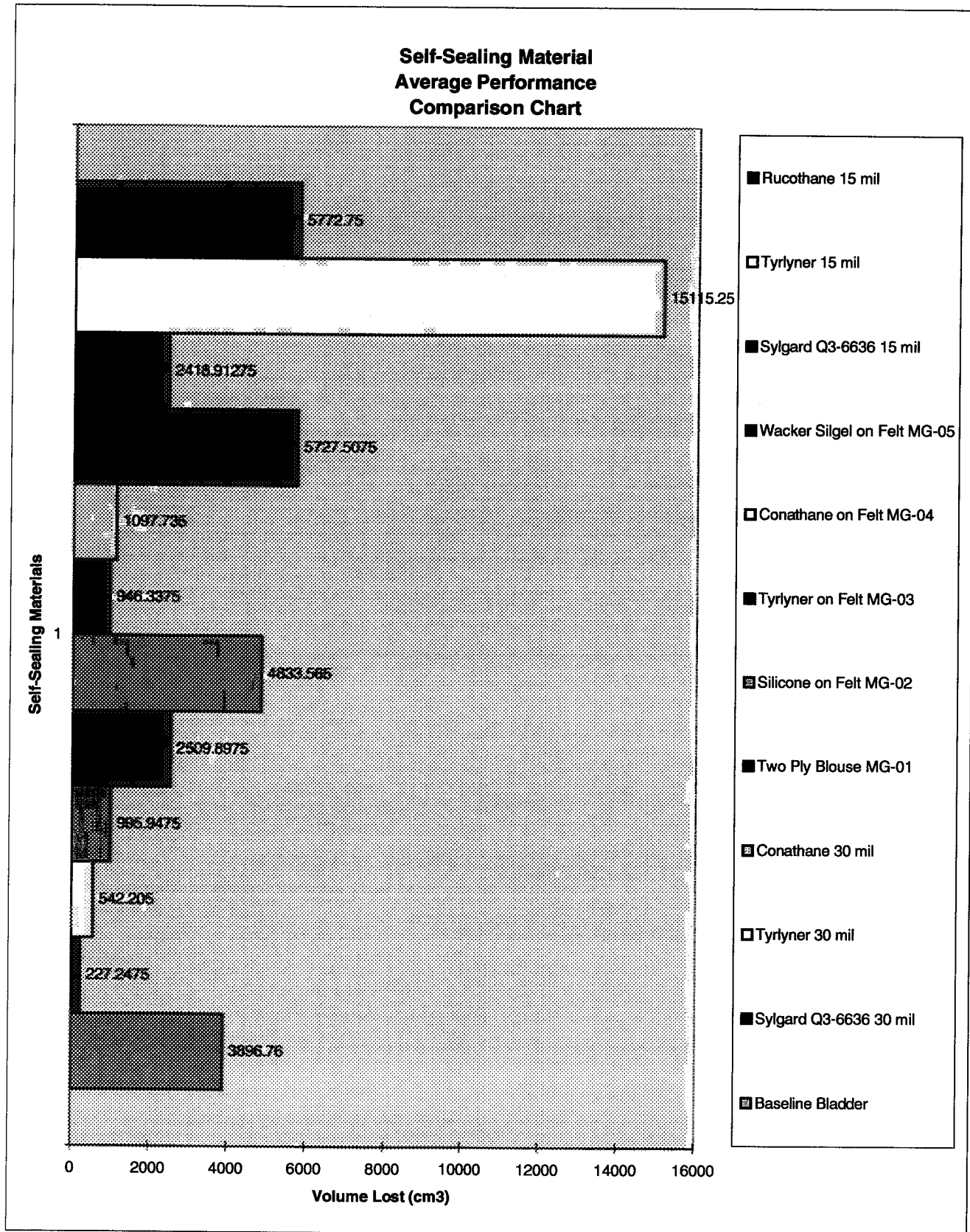


**Table 4**  
**Self-Sealing Material Trade Study**

#	Concept Description	Self-Sealing	Shelf Life	Mass	Durability	MATCO	Thermal Effects	Complexity in Mfg	Score	Notes
	1=worst, 10=best									
	Weighting Factor	1	0.7	0.9	0.6	1	0.7	0.8		
1	Baseline, Bladder	5	8	10	9	8	5	8	42.9	
2	Tyrlyner Urethane, 30 mil	9	6	5	6	2	4	5	30.1	
3	Sylgard Q3-6636, 30 mil	10	10	5	6	9	10	5	45.1	
4	Conathane EN-11, 30 mil	8	8	5	6	8	5	7	38.8	
5	MG-01-2-Ply Blouse	6	10	9	7	9	5	6	42.6	
6	MG-02-Silicone Vaccum Grease on Felt with Saran PVDC film	4	10	4	8	6	7	3	32.7	
7	MG-03-Tyrlyner Isocynate on Felt with Saran PVDC film	8	6	3	8	2	4	3	26.9	
8	MG-04-Conathane on Felt with Saran PVDC film	7	8	3	8	8	5	3	34.0	
9	MG-05-Wacker Silgel on Felt with Saran PVDC film	3	9	3	8	9	10	3	35.2	
10	Sylgard Q3-6636, 15 mil	6	10	7	4	9	10	5	41.7	
11	Rucothane, 15 mil	3	8	6	4	8	5	8	34.3	
12	Tyrlyner, 15 mil	1	6	6	4	2	4	5	21.8	

21

Note: MATCO - Material control testing includes tests for flammability, toxicity, thermal vacuum stability, and odor requirements

**5.1.8 Cold Flow Characteristics Test Method and Results**

Another characteristic important to determine, as it pertains to an end-use application of the self-sealing materials, is if the viscoelastic self-sealing materials possess a characteristic memory after being subjected to creasing under load. Due to an inordinate flexing requirement when in use, if cold flow problems were to exist, the self-sealing capacity of the pressure envelope would be compromised. To determine if this characteristic was present, one sample each of the Trylyner, Sylgard, and Conathane (30 mil) material lay-ups, were folded and placed under a 50 pound load, for one hour, at room temperature. Thicknesses of the fabric lay-ups were obtained at the fold immediately before the load was applied, and immediately after the load was removed. No change in the thickness of the creased line were noted. This initial evaluation represented that there were no short duration cold flow problems associated with these materials at room temperature.

**Table 5  
Cold Flow Characteristics**

	<b>Trylyner</b>	<b>Conathane</b>	<b>Silicone</b>
<b>Pre-load Thickness</b>	0.042 mils	0.036 mils	0.032 mils
<b>Average Immediate Post-load Crease Thickness</b>	0.043 mils	0.036 mils; some creasing of fabric substrate noted , but w/o separation	0.031 mils; some creasing noted in the fabric substrate without apparent separation

**5.1.9 Recommendations**

Further research and development on Silicone Polymers as a self-sealing layer will be required before integration into the SSA could occur. Two important areas where continued developmental efforts would be required include reduction of weight and thickness characteristics while maintaining an adequate self-sealing capability. Further study on manufacturing issues, cold flow properties, delamination potential, and thermal degradation would also be required.

**5.2 CUT, TEAR AND PUNCTURE RESISTANT MECHANISMS/MATERIALS**

The cut, tear and puncture resistance of fabrics are nominally similar in appearance, but actual mechanisms of deformation and failure are quite different. The failure mechanisms depend on the type of threat causing the rift in the fabric and the manner in which the yarns respond to the threat.

### 5.2.1 Puncture Mechanisms

In an event such as puncture, the threat is moving perpendicular to the plane of the fabric. There are two ways in which the penetrator can pass through the fabric:

1. The fibers/yarns move out of the way of the penetrator.
2. The fibers/yarns are ruptured to create a hole for the penetrator.

Depending on the shape of the penetrator, the frictional coefficient between the penetrator and the fibers, and the amount of available yarn/fiber movement, the particular failure mechanism will be identified. The scale of fiber motion is less than the scale of the yarn, typically on the order of several fiber diameters.

Considering an average fiber diameter to be 10-15  $\mu\text{m}$ , only a very small penetrator would be capable of moving the fibers around the penetrator to allow penetration to occur through fiber motion and friction. As illustrated in Figure 8, this motion requires space for fibers to move as well as some excess length of fiber or extension of fiber.

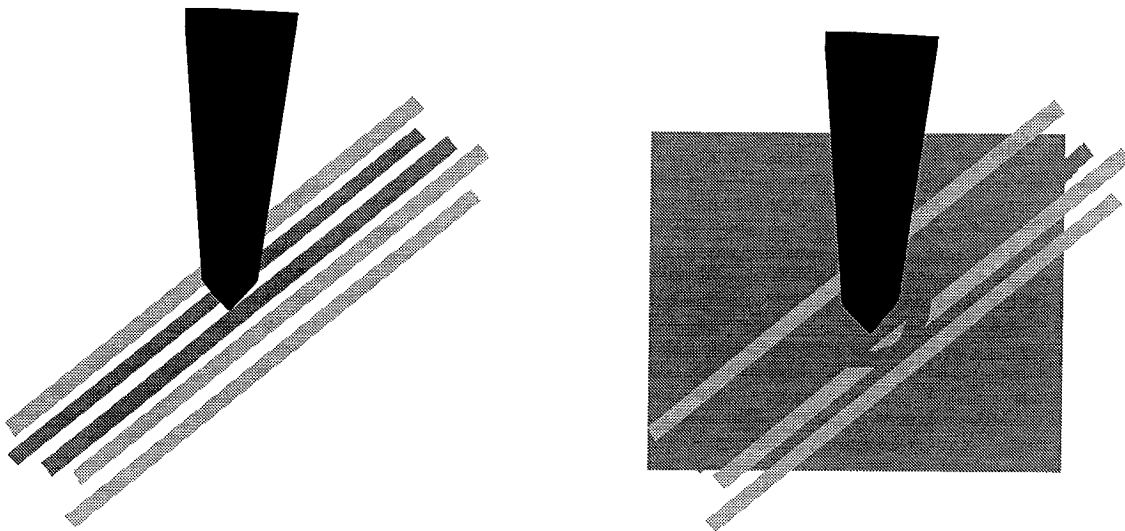


**Figure 8. Schematic Of Fiber Mobility Subject To Small Penetrator**

In the event that the penetrator is small compared to the yarn diameter, the penetration resistance is quite low. There may be some fiber failure from excessive strain, or from a compact yarn which does not allow much fiber failure. The failure would then occur as successive fiber failures. In the event of single fiber failure, the force required to cause failure depends on the particular fiber. In the case of high performance materials, fiber strengths are typically on the order of 50 cN. Even if several fibers break simultaneously, the maximum resistant force would be at most a few Newtons. The force-displacement curve would look like that shown in Figure 9.

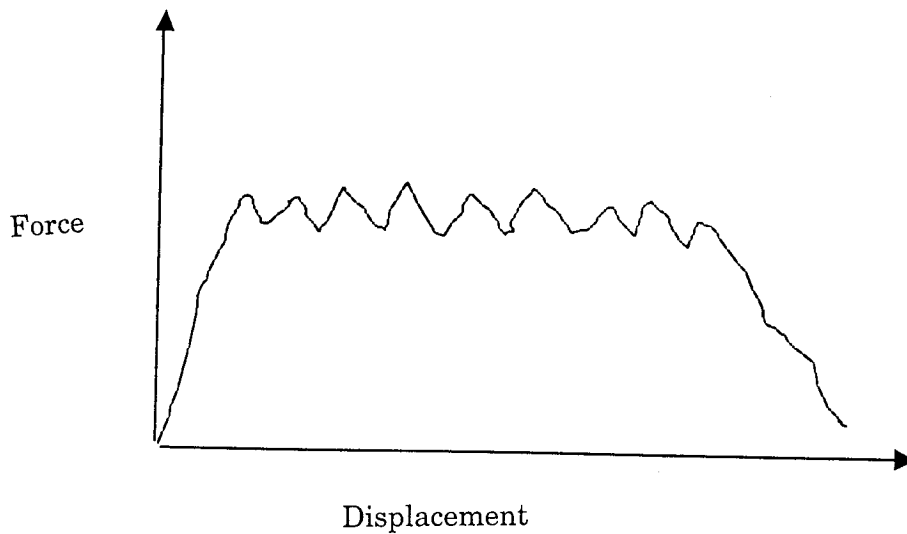


**Figure 9. Schematic Illustration Of Successive Fiber Failure From Small Penetrator**

However, when the penetrator diameter is on the scale of the yarn, the failure mechanism changes. In this instance, the yarn may move away from the penetrator or the yarn may rupture. In the case of yarn rupture, the failure load for a 840 denier Kevlar<sup>®</sup> yarn is on the order of 250 Newtons. The number of ruptured yarns can be estimated as the number of yarns ruptured in order to allow the penetrator to pass. At an upper limit, this would be:

$$P_p = d_p (e_w s_w^u L_w + e_f s_f^u L_f) / \cos b$$

Where  $P_p$  = the penetration force  
 $d_p$  = the diameter of the penetrator  
 $e_i$  = the number of yarns per unit length in the  $i$  direction  
( $i = w$  for warp direction,  $i = f$  for filling direction)  
 $s_i^u$  =  $i$ -direction yarn ultimate stress  
 $L_i$  =  $i$ -direction yarn linear density  
 $b$  = deflection angle of the fabric plane at the point of rupture

The distinction between yarn movement (resisting with perhaps a few Newtons) and yarn rupture (hundreds of Newtons) will depend not only on the diameter of the penetrator, but also the ability of yarns to move within the fabric.

If the fabric is loosely constructed so that the neighboring yarns have enough room to move around the penetrator, the penetration will occur at lower force levels. If the yarns are tightly packed so that the yarns cannot move to accommodate the penetrator, it will be necessary for the penetrator to rupture yarns to proceed.

Thus, to maximize the force required to cause penetration, it is useful to have a very tightly woven fabric with high strength yarns.

However, it needs to be pointed out that in the event of a penetration the tightly woven fabric will contain ruptured yarns which leave a permanent opening in the fabric. The fabric which is penetrated more easily will not rupture yarns, and the hole is more likely to close when the penetrator completes its path.

### **5.2.2 Tearing Mechanisms**

Tearing is the sequential or spontaneous breaking of yarns in a fabric, either singly or in small groups, along a line through the fabric. Typically the yarns being broken are transverse to the principle load direction. Tearing can occur as a result of a steadily increasing load or as an equivalent to crack propagation in a prestressed fabric.

Similar to the discussion on penetration, tearing is affected by the yarn's ability to move within the fabric. When the yarns cannot move at all, the tear propagates by sequential individual yarn failure. The tear strength can be predicted as the strength of a single yarn.

If there is some yarn motion, one yarn may slide within the fabric until it meets another, and the tear cannot propagate until two yarns are bunched together. The tear strength doubles in this case. As shown in Figure 10, the mobility of the yarns within the fabric dictate the tear strength of the fabric

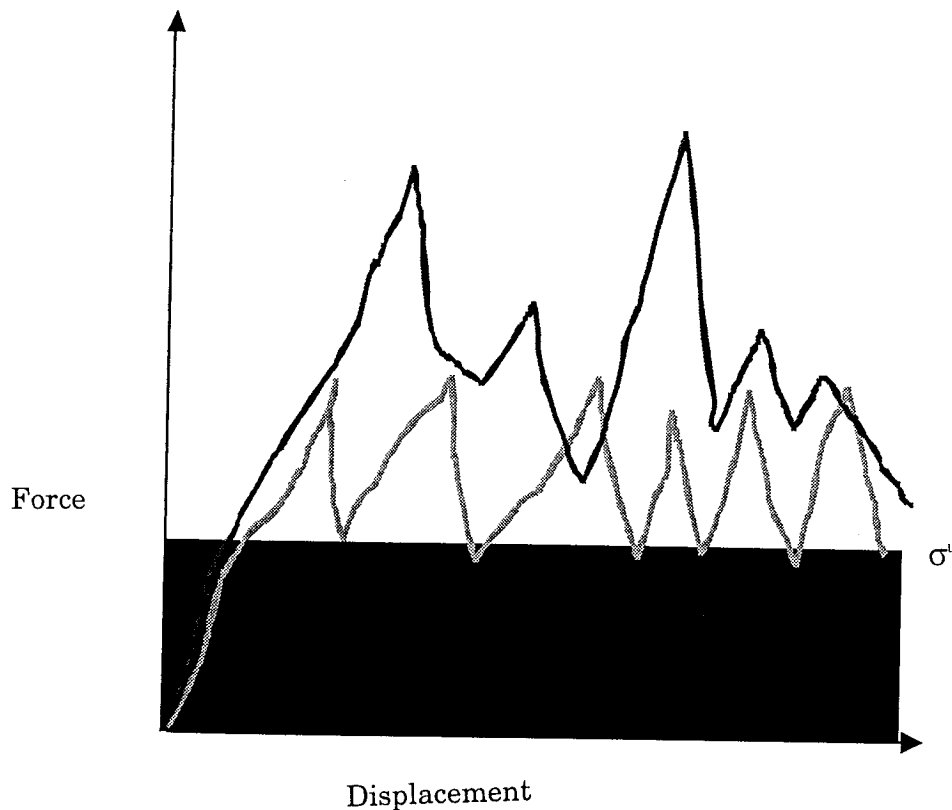


**Figure 10. Schematic Illustration Of Tear Resistance For Varying Degrees Of Yarn Mobility.**

Gagliardi and Nusselle developed the following relation for tear strength, which was later supported by Hager et al.:

$$T = \frac{m\sigma''\epsilon''}{2} + b$$

Where

T = fabric tear strength

$\sigma''$  = fabric tensile strength (ravel strip)

$\epsilon''$  = fabric strain to failure

m = slope fabric relating fabric toughness to tear resistance

b = constant depending on fabric construction

In further studies by Gagliardi and Grunfest, fabrics were treated with finishing resins which reduced yarn extensibility, increased yarn tensile modulus, and had little effect on yarn strength. They found that this decreased fiber capacity for energy absorption and also the ability of the yarns and fabrics to resist tearing.

From this it can be seen that for an uncoated fabric, the tear resistance of the fabric increases with increasing yarn strength and yarn extensibility. This further suggests that yarn twist should be applied in such a manner as to increase the strength of the yarn. For a continuous multifilament yarn, zero twist is optimum. For a staple yarn, twist should be applied to the optimum twist level.

An exception to this design criteria is found for coated fabrics. In this case, infiltration of coating material will increase tear strength, and subsequently it is occasionally beneficial to twist multifilament yarns because the fabric is thicker, so the amount of applied coating is greater.

The greater the yarn mobility, the greater the tear resistance because multiple yarns must be ruptured at the same time.

Considering the importance of yarn mobility, Teixeira et al. looked at the performance of fabrics with a variety of weave constructions. They found that for fabrics made with the same warp and filling yarns, and same end and pick counts, the tear resistance depended on weave structure in the following order:

1. 3-4 basket
2. 2-2 basket
3. 2/2 twill
4. 4 harness satin
5. plain weave

### **5.2.3 Cutting Mechanisms**

The mechanism to cut combines both the puncture and tearing mechanisms. The process variables occurring to resist this event are influenced by the polymeric structural formation of high strength fibers, the diameter of the cutting edge, the compressive moduli of the fiber/yarn, and very significantly, the amount of yarn movement allowed from the fabric's construction parameters.

### **5.2.4 Fabric Design**

Following the above design guidelines, fabric were chosen to have high strength, good yarn mobility, but relatively stable weave structure. Plain weave fabrics were formed to compromise good coverage and abrasion resistance with decent tear and cut resistance.

Kevlar<sup>®</sup> and PEN<sup>®</sup> yarns were used in the production of the fabrics. Hybrids were also formed. Of the four fabric samples selected for evaluation in this study, a summary of the construction variables are indicated in Table 6.

**Table 6**  
**Overall Fabric Construction Parameters**

Fabric Sample	Yarn Direction	Yarn Composition	Yarn Denier	Yarn Count	Fabric Constructions
A	warp	Pentex	1000	32	plain weave
	fill	Pentex	1000	18	
B	warp	Pentex	1000	32	plain weave
	fill	Kevlar	1500	18	
C	warp	Pentex	1000	32	plain weave
	fill	Pentex Kevlar 29	3-1000 1-1500	18	
Incumbent - face	warp	Gore-Tex	400	52	plain weave
	fill	Gore-Tex	400	43	
Incumbent - back	warp	Nomex Kevlar 29	200 400	39	ripstop
	fill	Nomex Kevlar 29	200 400	34	

**5.2.5 Puncture Resistance Testing Methods And Results**

*Test Method*

In Puncture Resistance Testing, a fabric sample is mounted to a stationary support assembly of a tensile tester, and a puncture probe, of set dimensions is mounted to the compression cell. The puncture probe is lowered toward the material specimen, at a constant velocity, until puncture occurs. The force required to puncture the fabric is measured by the compression cell. Elongation (or deflection) of the specimen prior to puncture is also measured. The reported value is the average of twelve test replicates, with three replicates for each of the four material specimens tested.

*Test Results and Discussion*

**Table 7**  
**Puncture Resistance Testing Results**  
**(ASTM F 1342 - 91)**

Sample	Fabric Weight	Load Range (lbs)	Cumulative Avg.	Std. Deviation
A	7.11 oz/yd <sup>2</sup>	0.4 - 2.5	1.3	0.7
B	7.83 oz/yd <sup>2</sup>	0.5 - 4.7	1.7	1.2
C	11.51 oz/yd <sup>2</sup>	0.3 - 2.3	1.1	0.6
Incumbent Fabric	15.69 oz/yd <sup>2</sup>	1.8 - 4.0	2.8	0.6

There is a significant variance in fabric construction between the incumbent fabric and the prototypes which would account for the higher puncture load that the incumbent fabric was able to withstand.

The incumbent fabric is of a double-cloth construction where two separately structured fabric layers are constructed as one. Both of these layers possess a higher number of yarns in a given area than do any of the single-layered prototype fabrics. In these fabric samples, the higher yarn count of the incumbent fabric equates to a more compact interlacing and a more dense fabric covering. This relationship reduces fabric porosity and allows for a better resistance to a puncture probe. If on the other hand, the materials in Samples A through C were woven similarly their corresponding load requirements for puncture creation would increase substantially.

## **5.2.6 Cut Resistance Testing Methods And Results**

### *Test Method*

In Cut Resistance Testing, a fabric sample is mounted on a mandrel and is cut by a blade at a constant rate of speed. The load, when applied to the blade, and ultimately onto the fabric sample, allows for the determination of a cut-through distance when the blade makes electrical contact with the mandrel and disengages the motor.

Blade dulling is an important variable to consider in this test procedure and therefore, are used only once, to produce one cut. In order to standardize the variability found in different blades, a correction procedure is included in the process which involves measuring the cut distance on a standard rubber, under standard load.

Five cut distances, at each of three loads were obtained that cause cuts in three different distance ranges. Those ranges include: 5 - 20 mm, 21 - 32 mm, and 33-50 mm. A curve, representing the cut resistance to the applied load is then constructed. Ideally, these curves are exponential in shape, so the data are curve fitted to an exponential curve and the load required to cause a cut in 25 mm of blade travel is interpolated from the exponential regression. This value is the reported cut resistance of the sample. Additionally, the correlation coefficient for the exponential fit is often reported. (Thomas, 1998)

### *Test Results and Discussion*

Samples A and C require the highest application of load to create a cut, and therefore, possess the highest cut resistant properties. This is due primarily to the fibrous constituents of these materials and these prototypes demonstrate the positive result of weight reduction compared to the current fabric. These results also indicate that fabric weight is not a determining factor to cut resistance as are fabric constituents and method of construction. Any variance noted could be attributed to the location of the blade on the fabric's surface when the load is

applied. Depending on the where on any given yarn the blade lands, the result may show more or less a resistance to cutting. In the case of Sample B, there is more Kevlar 29® per area than any of the other fabrics, and that may account for the overall lower load required for cutting. This may be due to the significantly lower compressive modulus that the Kevlar possess than that of the PEN.

**Table 8**  
**Cut Resistance Testing Results**  
**(ASTM F 1790-97)**

Sample	Fabric Weight	Interpolated Wt. (g)	R <sup>2</sup> Value
A	7.11 oz/yd <sup>2</sup>	674.0	0.831
B	7.83 oz/yd <sup>2</sup>	502.0	0.860
C	11.51 oz/yd <sup>2</sup>	675.0	0.846
<b>Incumbent Fabric</b>	15.69 oz/yd <sup>2</sup>	379.0	0.956

**5.2.7 Cut And Puncture Recommendations**

An improved resistance to cut and puncture threats could be achieved in the prototype fabrics through an optimized fabric construction. Areal density of the fabric can be increased through the incorporation of a more tightly woven fabric. Methods to achieve this end include, an increased degree of fiber/yarn packing, adjustments in the yarn diameters used, and development of a multilayered fabric with varying methods of interlacing which would promote different fabric performance properties.

**5.3 HYPERVELOCITY IMPACT**

**5.3.1 Background**

There have been reports of occurrences where the integrity of the space suit was threatened by cuts and/or punctures. Now, rapidly increasing levels of debris found in the space environment are also threatening the level of protection that the space suit can provide. Probability models of space suit survival have indicated that increased levels of protection against these threats will be required from the space suit near the year 2000 (Hodgson, 1993). The EVA hazards associated with MMOD impact is directly related to the ability of the impacting particle to penetrate the space suit and create a leak. These hypervelocity impacts have two defining characteristics. The first is that at the moment of collision, the velocities of the colliding materials are greater than the speed of sound and the energy released on impact is large compared to the heat of vaporization. As a result, intense shock waves pass through the materials, resulting in fragmentation and melting, (Whipple Effect). At sufficiently high impacting velocities, some of the impacting material may be vaporized. In a material composed of multiple layers and/or one which possesses sufficient thickness, such as the SSA, further fragmentation and destruction can occur.

At the velocities (8.0 - 17.0 km/s) and accelerations involved in these events, the effects of material mechanical properties such as yield and ultimate strength are often minimal. Material densities and the energy released in the impact (kinetic energy of the incident particle) are the dominant factors. This is reflected in the following expressions:

$$t_p = 0.655 * (1/E)^{.125} * (r_M/r_T)^{.5} * VM^{.875} D_M^{1.055}$$

$$t_p = 9.2 * (BH)^{-.25} * (r_M/r_T)^{.5} * (V_M/c)^{.667} * D_M^{1.06}$$

Where:  $t_p$  = the maximum thickness penetrated

$E$  = the percent elongation of the target material at failure

$r_M$  = the density of the incident particle

$r_T$  = the density of the target material

$V_M$  = the incident velocity of the particle

$D_M$  = the diameter of the particle

BH = the Brinell Hardness of the target material

$c$  = the speed of sound in the target material

In comparison to the cut resistance of a material, the material's structural properties (percent elongation and Brinell Hardness) have relatively little effect on the impact penetration depth in comparison to the particle and target densities, the collision velocity, and the size of the incident particle. These relationships, agree that equivalent damage to a given target will result from different impacts in which the kinetic energy of the impacting particle is the same. (Hodgson, 1993)

The damage caused from hypervelocity impact is a hole and a debris cloud where the diameter of the hole generally exceeds the diameter of the incident particle by less than a factor of two. The debris cloud created from impact will spread will spread over an area which grows in proportion to the intervening distance and typically exhibits a cone angle of 30 to 50 degrees. Therefore, multiple fabric layering effects are important for EVA in terms of understanding present risks and potential shielding improvements. In the TMG, this whipple effect has been addressed through of multiple layering of reinforced Mylar® on almost all exposed surfaces. This lightweight approach to micrometeoroid and orbital debris shielding will spread any impact over a sufficiently large area to prevent penetration of subsequent layers.

Impacts occurring at angles off the normal, create ricocheting scenarios and/or secondary particles. Laboratory testing has demonstrated that impacts at an incidence more than 45° off the normal produce potentially damaging secondary particles in significant quantity. Formed from both fragmentation of the primary particle and from material removed from the surface at the time of impact, they spread from the point of impact over approximately a 30° angle to either side of the incident particle's line of flight and above the tangent to the

surface. Measurements of craters formed by impacting secondaries in a laboratory witness plate have estimated that the largest and most damaging of these secondary particles may be half the mass of the incident primary, and that they move at velocities on the order of 30% of the original primary particle's velocity. (Hodgson, et al., 1993) Subsequently, the baseline and prototype fabric constructions were sent to NASA Johnson Space Center for Hypervelocity Impact Testing.

### **5.3.2 Hypervelocity Testing Method And Results**

#### **5.3.3 Hypervelocity Impact Test Method**

SSA Material lay-ups were constructed at ILC Dover and sent to NASA JSC for Hypervelocity Impact Testing (HVI). The lay-ups were constructed in the same sequence as the SSA. The outermost layer of the lay-up consisted of either the down-selected prototypes or the incumbent Ortho-Fabric. Each material lay-up was installed inside the 0.17 caliber target chamber. A 0.040 inch thick aluminum witness plate was installed 2 inches behind the rear face of the SSA lay-up and once the sample lay-up was mounted, the target chamber was evacuated to 100-200 microns. The sample lay-ups were impacted by aluminum projectiles at of varying size, velocities, and impact angles.

#### **5.3.4 Hypervelocity Impact Test Results And Discussion**

Criteria for failure was predetermined to be with the occurrence of bladder penetration. Determined post-test, by visual examination of the polyurethane-coated nylon bladder and of the witness plate. A summary of the preliminary hypervelocity impact test results are found in Appendix F which delineate each fabric's performance.

The samples submitted as single layer, plain weave prototypes showed a similar, if not slightly improved performance response in HVI Resistance over the incumbent fabric. The most positive results for HVI resistance of the prototypes were identified from Sample A. Damage resulting to the subsequent fabric layers is representative of the increased energy absorption at the initial prototype fabric layer. With a projectile diameter of 0.5 mm, the fabric lay-up was able to resist complete penetration. A microscopic evaluation at the location of the stained area of bladder cloth is required to quantify the extent of damage to the coated layer. When the projectile diameter was increased to 0.6 mm, there was a small penetration, which if incorporated with a self-sealing layer, would pose no immediate threat to the astronaut. When the projectile was decreased to 0.4 mm, the examination of Sample A revealed that the initial fabric layers penetrated showed less damage than those of the Incumbent Fabric but the final fabric layer (the bladder) was penetrated. Given these preliminary results, adjustments to the fabric construction of Sample A, by the way of an increasing the given area of yarn coverage would work to improve these results even more. One method of increasing the fabric coverage and dramatically increasing the protection to HVI while remaining below the current weight

requirement would be to reconstruct the PEN into a similar doublecloth configuration as is the current TMG.

### **5.3.5 Recommendations**

In an attempt to optimize the HVI performance results, the fabric lay-ups were rearranged allowing for two consecutive layers of Prototypes A and B. Though not exact in its replication of the doublecloth construction found in the incumbent fabric, it was hoped that additional impact resistance could be attained. At the time of publication of this report, these results are still pending. The results will be submitted as an Addendum to this report.

At the time of the publication of this report, two of the most promising 30 mil self sealing Sylgard Q3-6636 samples were submitted for unpressurized hypervelocity impact testing. They will be placed in a fabric lay-up and located adjacent to the bladder cloth, facing outward. The two fabric lay-ups in which they will be included will have Prototype A and the incumbent Ortho-Fabric as the outer most TMG layer. This testing will help determine if the self sealing layer will improve resistance to MMOD impact, and a visual description and quantification of the damaged incurred to the seal sealing testing will be achieved post testing. These results will be submitted as an Addendum to this report.

## 6.0

### CONCLUSIONS

Through this research effort, significant knowledge of materials and technologies have been gained to state unequivocally that substantial enhancements for to the SSA can be incorporated to improve the TMG cut and puncture resistance, HVI resistance, and self-sealing mechanisms that the space suit now provides.

The increased frequency of EVA work that will be associated with the construction and habitation of the Space Station, as well as that which will occur with future lunar/mars missions necessitate that enhancements such as this occur.

An improved cut resistance can be built into the outermost layer of the TMG by using the recently developed polymer, polyethylene naphthalate. With adjustments to this fabric's construction parameters, the puncture resistance can also be improved substantially. The adjustments made to the fabric construction, enhancing the cut and puncture resistance, will also result in an improved resistance to the constant threat of hypervelocity impacts.

If the outer protective layers of the space suit are penetrated, a self-sealing layer can be incorporated to seal puncture sites. A single layer of silicone gel, Sylgard Q3-6636, performed the most consistently of all candidates examined.

## 7.0

### RECOMMENDATIONS

In order to achieve the goals and objectives set forth in this effort, which were to incorporate enhanced performance capabilities for the SSA, the following steps are recommended for completion:

#### *Self-Sealing Capabilities*

- Continue efforts to optimize self-sealing weight and thickness characteristics.
- Perform Hypervelocity Impact Testing on the self sealing material at the optimized weight and thickness.
- Evaluate the cold flow characteristics of the selected self-sealing material through the range of temperatures to which it would be exposed.
- Evaluate thermal degradation characteristics of the selected self-sealing material.
- Evaluate the manufacturing issues of a self-sealing layer which will impact design parameters.
- Send the selected fabric to White Sands Testing Facility for Material Control Testing for Flammability, Toxicity, Thermal Vacuum Stability, and Odor.

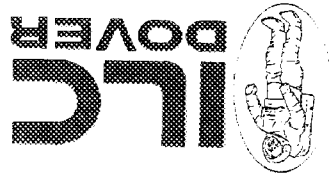
#### *Cut, Puncture, and Hypervelocity Impact Resistance Characteristics*

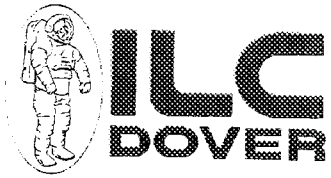
- Isolate the most effective fabric construction parameters for the outermost layer of the TMG.
- Send the selected fabric to White Sands Testing Facility for Material Control Testing for Flammability, Toxicity, Thermal Vacuum Stability, and Odor.

**APPENDIX A**  
**SELF-SEALING CONCEPTS SUBMITTED FOR EVALUATION**

Moishe Gartinkle and Chris Pastore  
Philadelphia College of Textiles and Science

# Self-sealing concepts





# Liquid Sealant Concepts

---

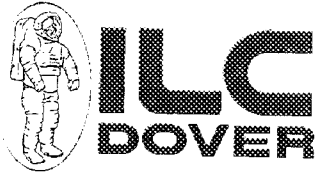


- ❁ Quilted Sealant

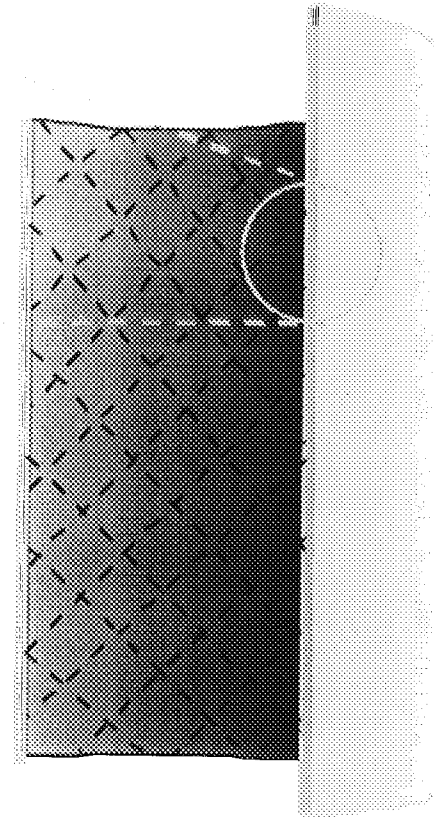
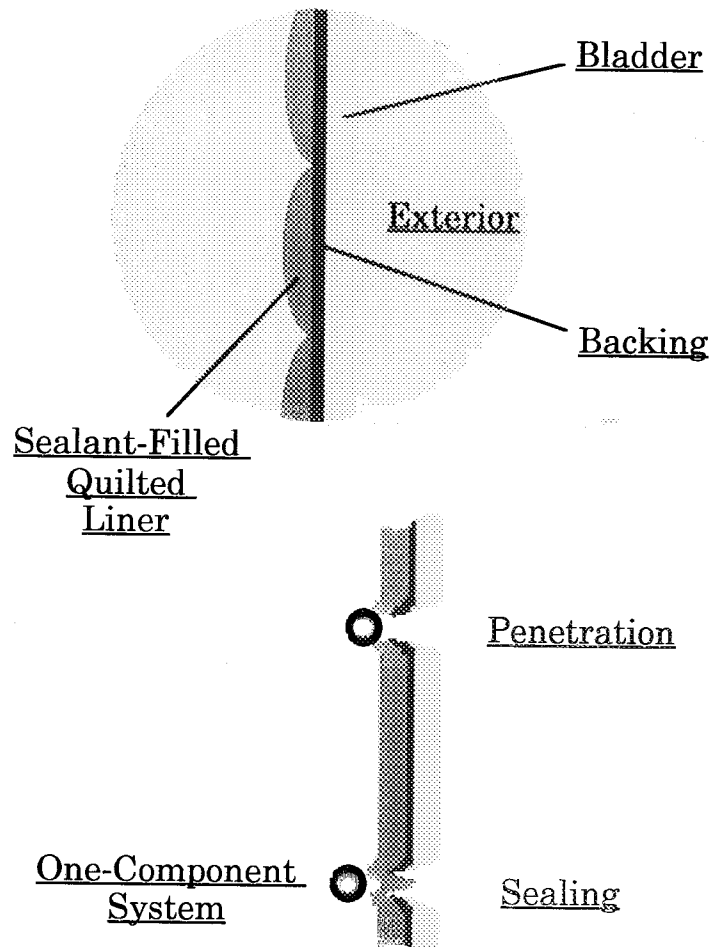
- ❁ quilted layer incorporates sealant near bladder

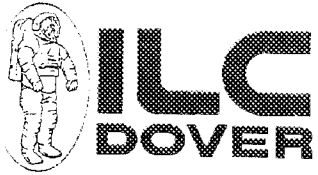
- ❁ Impregnated Felt

- ❁ layer of felt holds sealant stable near bladder

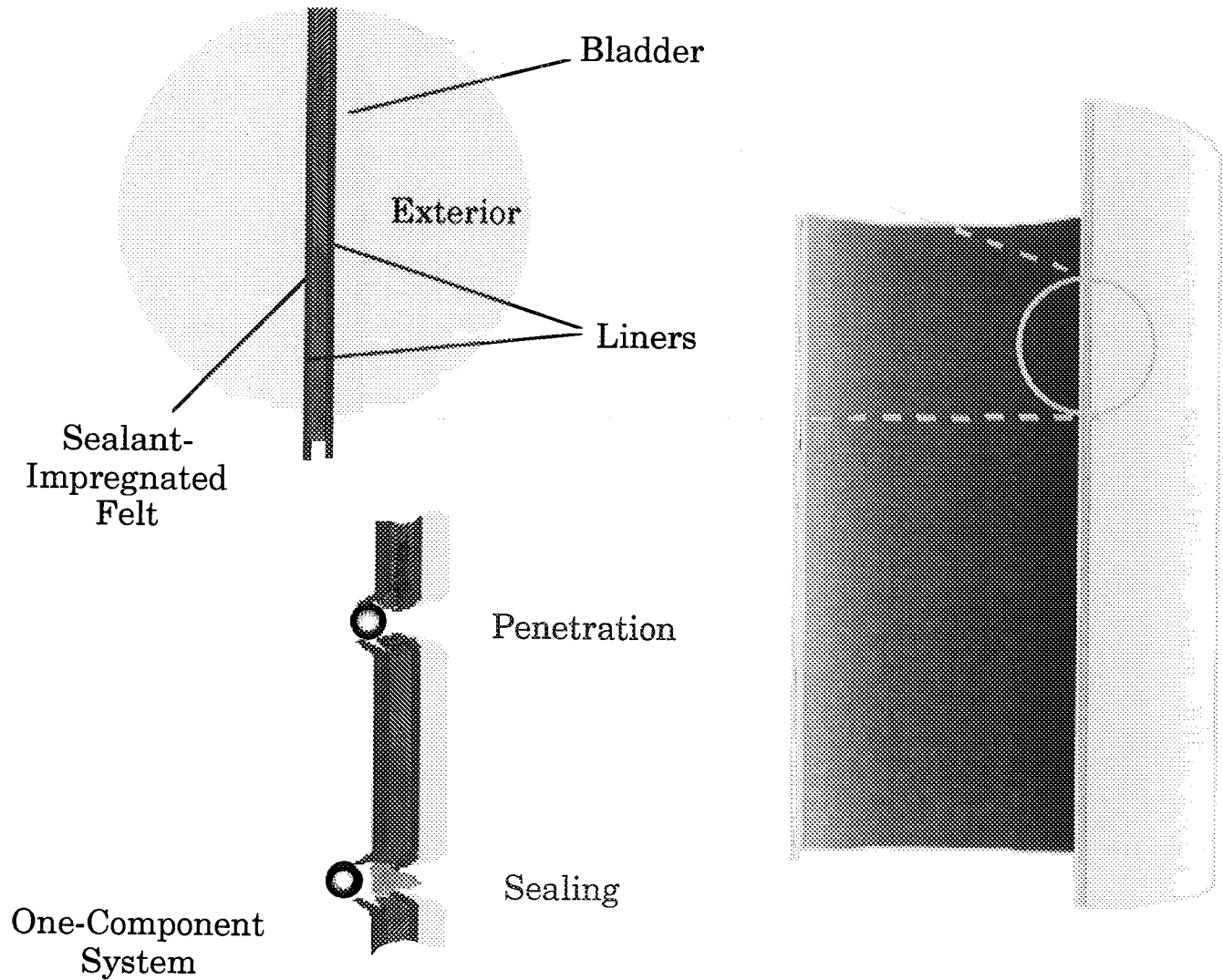


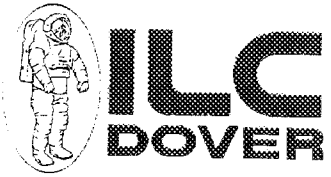
# Quilted Sealant





# Impregnated Felt





# Foaming Concepts

---

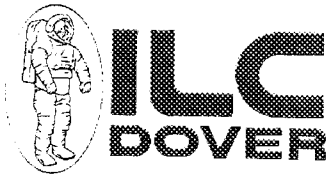


## ❁ Filled Fibers

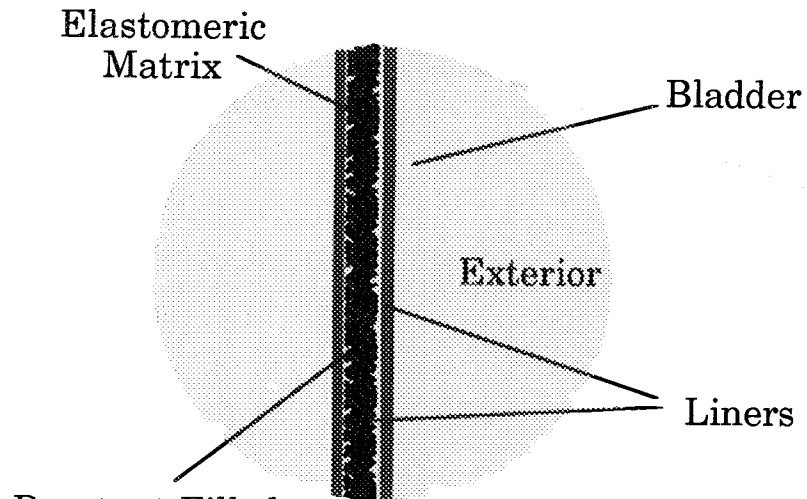
- ❁ hollow fibers filled with foaming reagents form layer/fabric. When ruptured, reagents mix and react to seal.

## ❁ Embedded Capsules

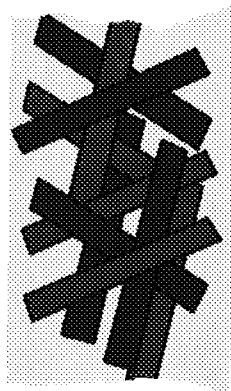
- ❁ micro-encapsulated foaming reagents embedded in elastomer. When ruptured, reagents mix and react to seal



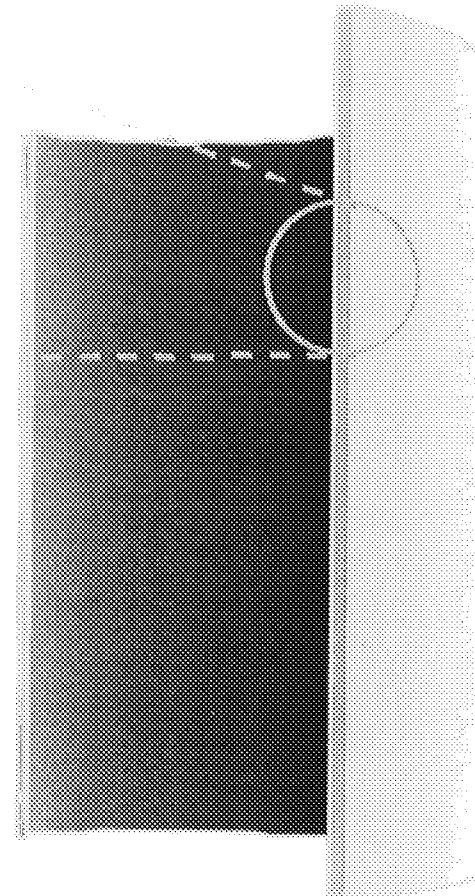
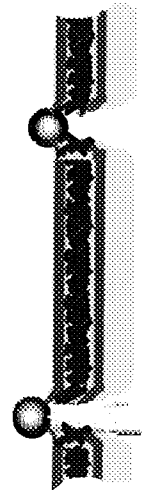
# Filled Fibers



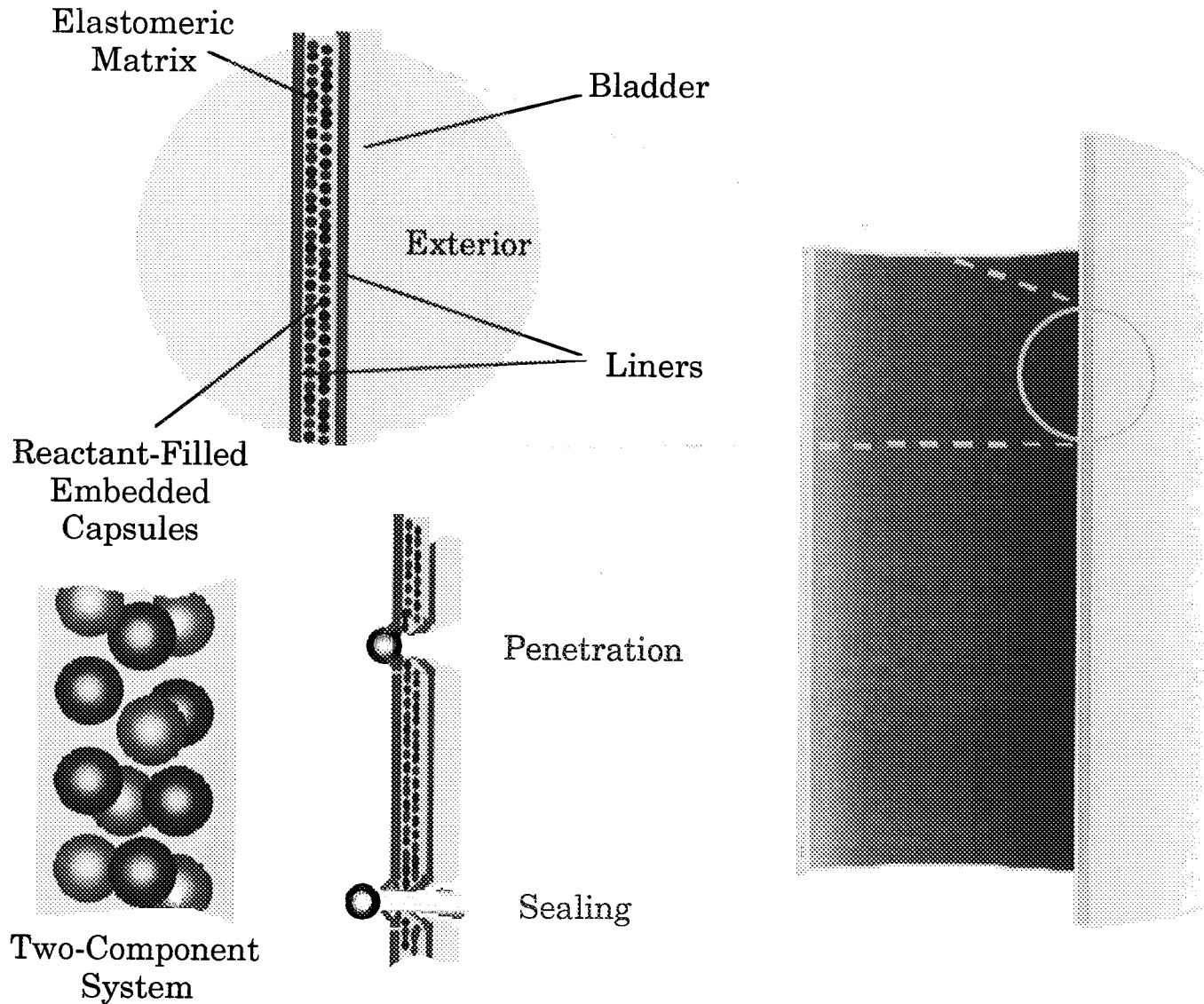
Reactant-Filled  
Hollow  
Fibers



Two-Component  
System

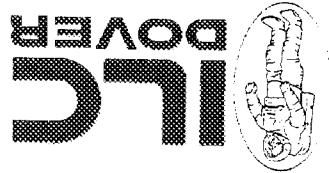


# Embedded Capsules



## ✿ Blousy Fabric

- ✿ Oversized blousy fabric is beneath bladder. When ruptured, air flow pulls fabric through puncture.

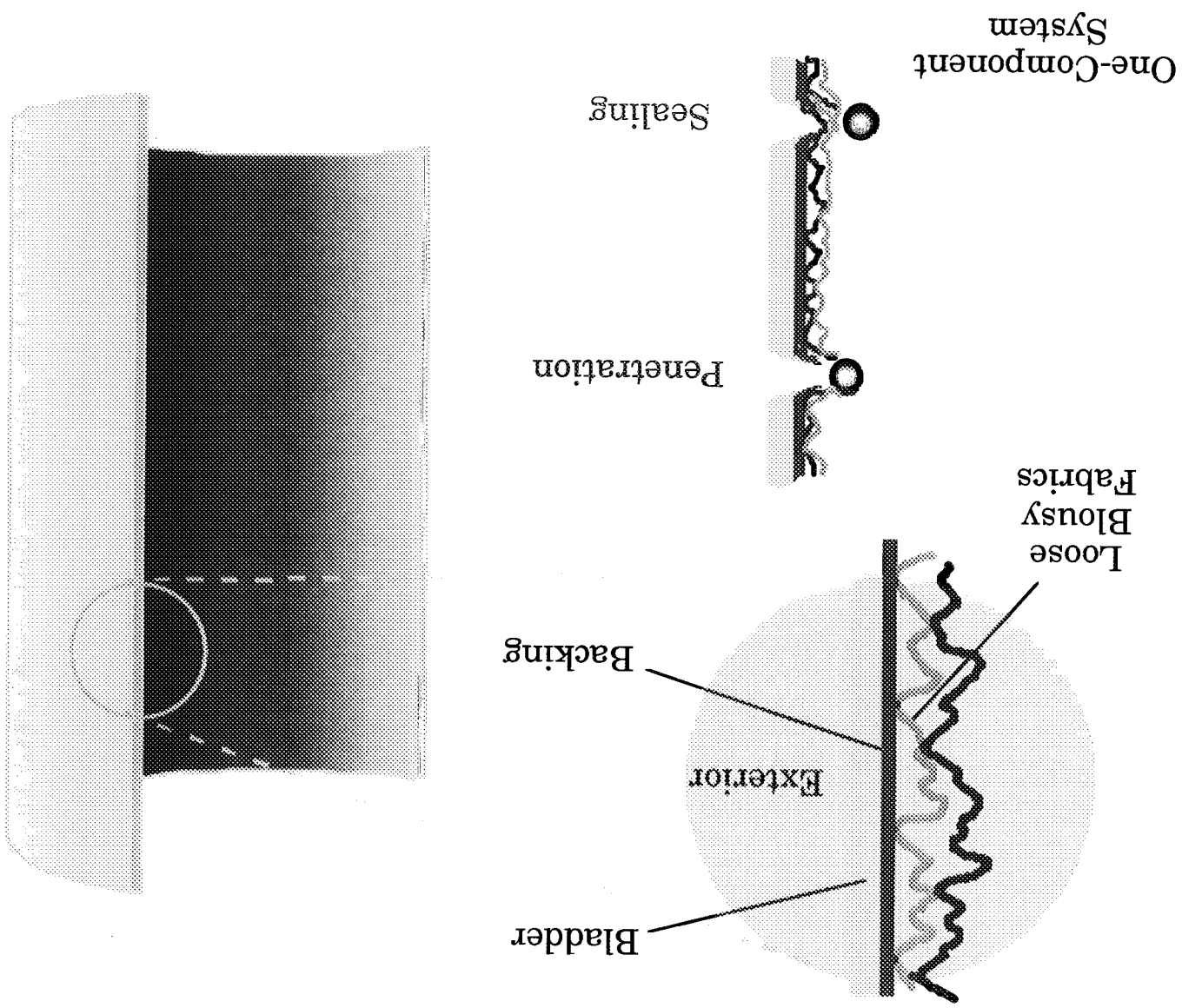


---

# Mechanical Sealant

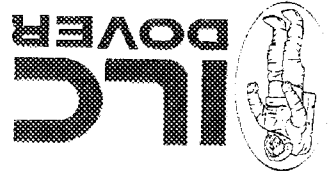


# Blousy Fabric



## ✿ Reactant Layer

- ✿ Low viscosity elastomer rapidly increases in viscosity when exposed to moisture.



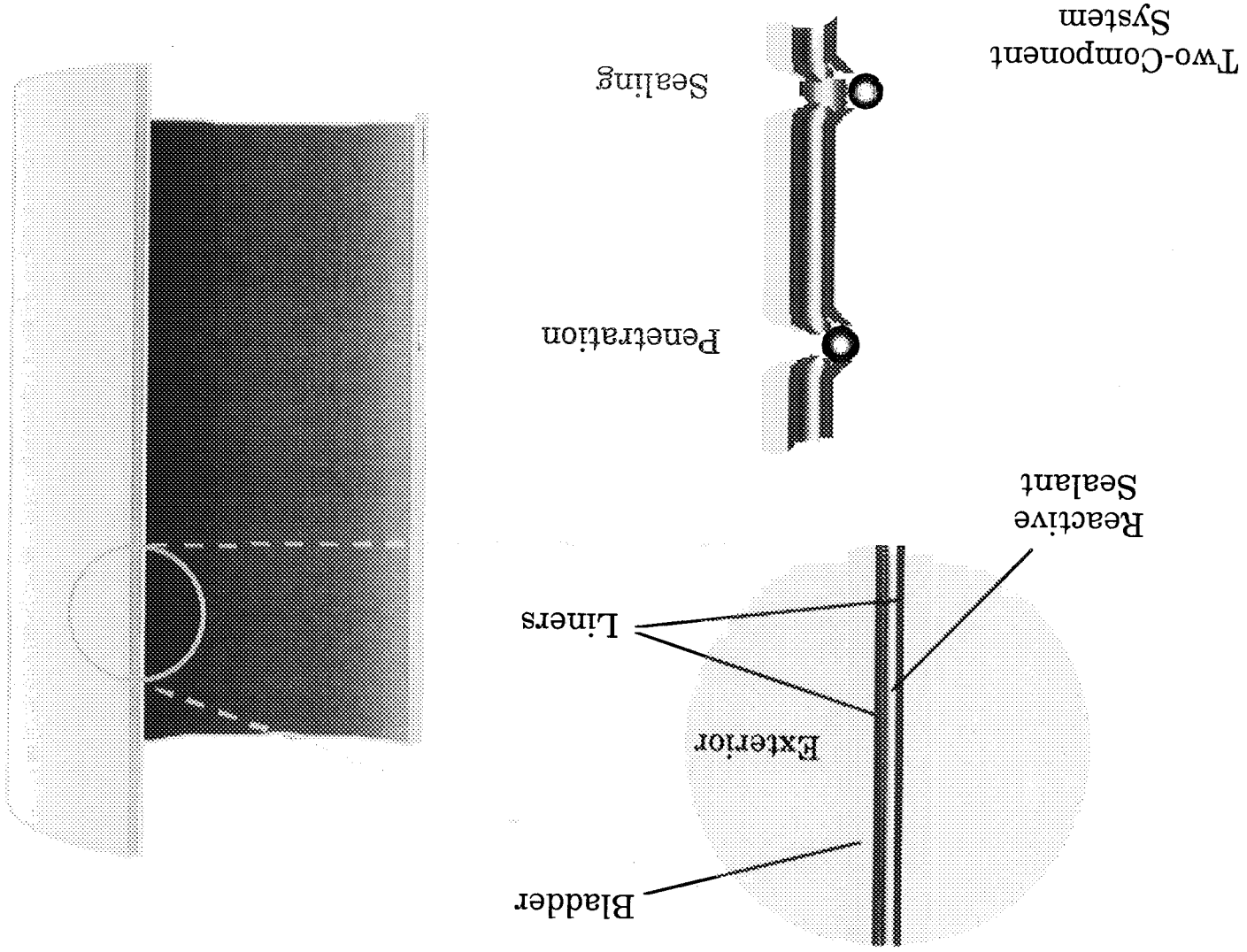
---

## Environmental Response





# Reactant Layer

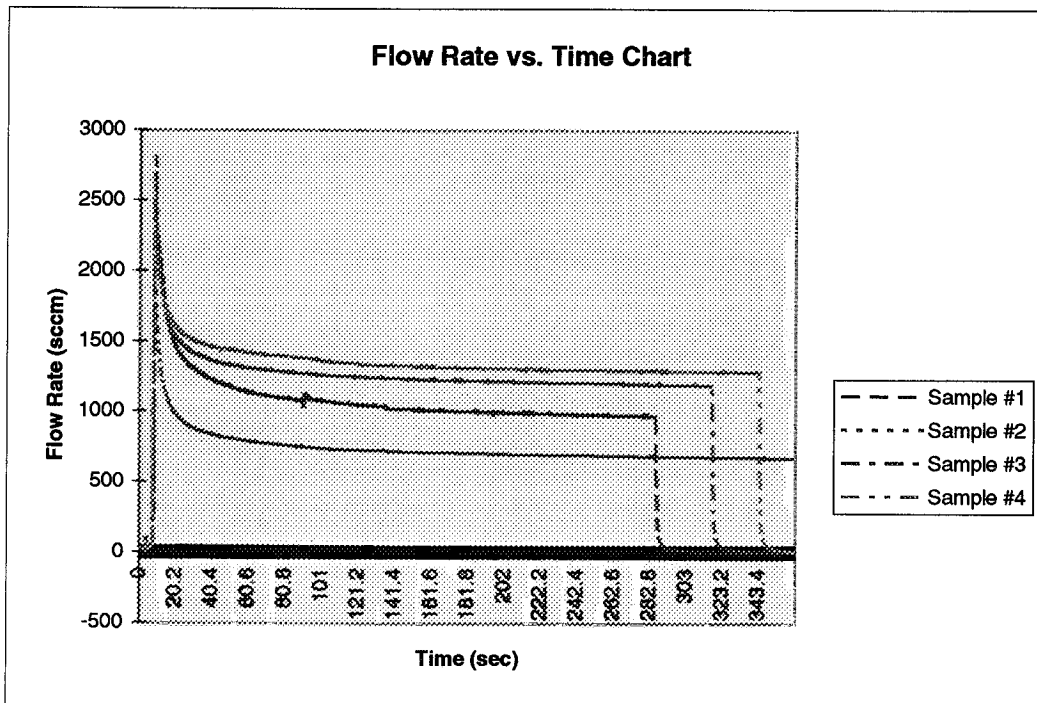


**APPENDIX B**  
**LABORATORY ANALYSIS REPORT, SELF-SEALING PERFORMANCE TESTS**

**Laboratory Analysis Report  
Self-Sealing Performance Test**

Test Method	1275-70001	Sample Run		Weight of Sample Specimen (gm)		Average Initial Pressure (Pa)		Average Initial Flow Rate (sccm)	
Log No.	8021-01	1	4.74	29440.6	22.44				
Work Order No.	1275-17039	2	4.67	29854.3	23.17				
Material	Baseline, Bladder	3	4.73	29992.2	23.64				
Probe Used	Puncture Probe	4	4.71	29785.4	24.62				
Thickness (cm)	0.0289	Cum. Avg	4.71	29768.1	23.47				
Weight	See Table	Cum. Std Dev	0.02	163.76	0.66				
Date	May 12, 1998								

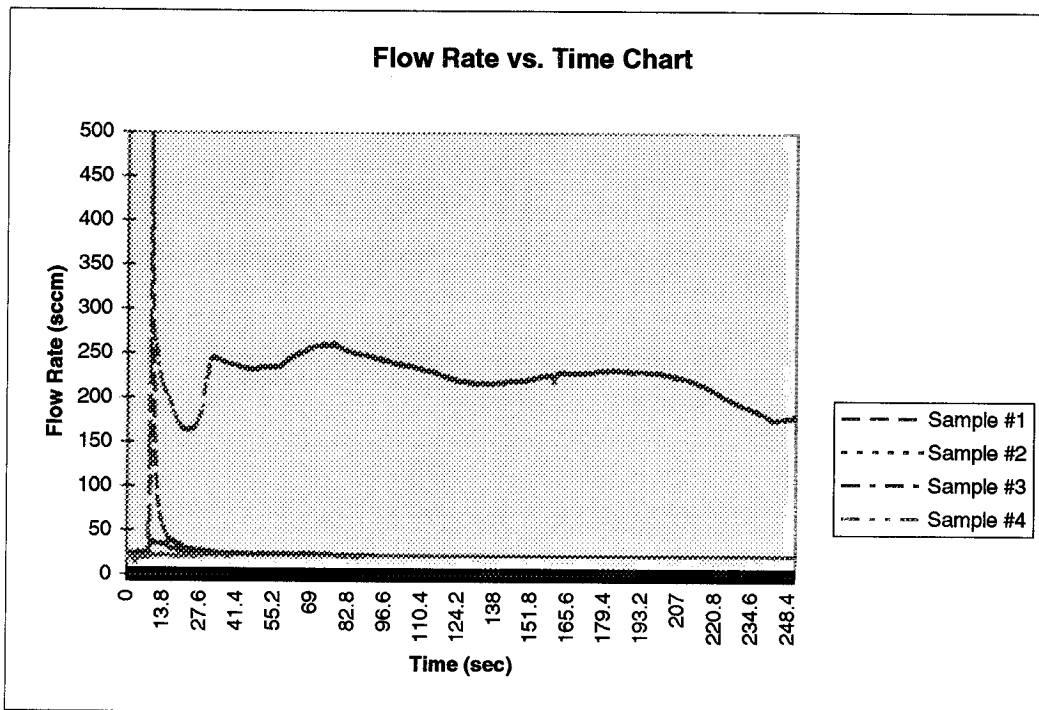
Sample Run	Max. Load (N)	Min. Pressure after Puncture (Pa)	Max. Flow Rate (sccm)	Min. Flow Rate after Puncture (sccm)	Delta Flow Rate Max. (-) Min. (sccm)	Delta Flow Rate Min. (-) Initial (sccm)	Change of Time from Max. to Min. Flow Rate (sec)	Volume Lost in 180 sec After Max. Flow Rate (cm <sup>3</sup> )
1	51.93	28302.9	2803	973	1830.11	950.56	360.00	3802.89
2	55.42	28891.8	1875	676	1198.90	652.83	300.00	2632.08
3	49.20	28936.6	2625	1190	1435.43	1166.36	267.00	4399.42
4	49.45	28831.8	2302	1287	1015.20	1262.38	275.00	4752.65
Cum. Avg	51.50	28740.8	2401	1032	1369.91	1008.03	300.50	3896.76
Cum. Std Dev	2.18	218.94	312.86	207	262.86	206.34	29.75	679.28



**Laboratory Analysis Report  
Self-Sealing Performance Test**

Test Method	1275-70001	Sample Run	Weight of Sample Specimen (cm)	Average Initial Pressure (Pa)	Average Initial Flow Rate (sccm)
Log No.	8021-01	1	22.68	29481.7	23.08
Work Order No.	1275-17039	2	23.85	29529.9	21.00
Material	Sylgard Q3-6636, 30 mil	3	24.30	29426.8	19.28
Probe Used	Puncture Probe	4	23.79	29572.4	20.02
Thickness (cm)	0.0911 Dev 0.0016	Cum. Avg	23.66	29502.7	20.85
Weight	See Table	Cum. Std Dev	0.49	48.43	1.19
Date	May 14, 1998				

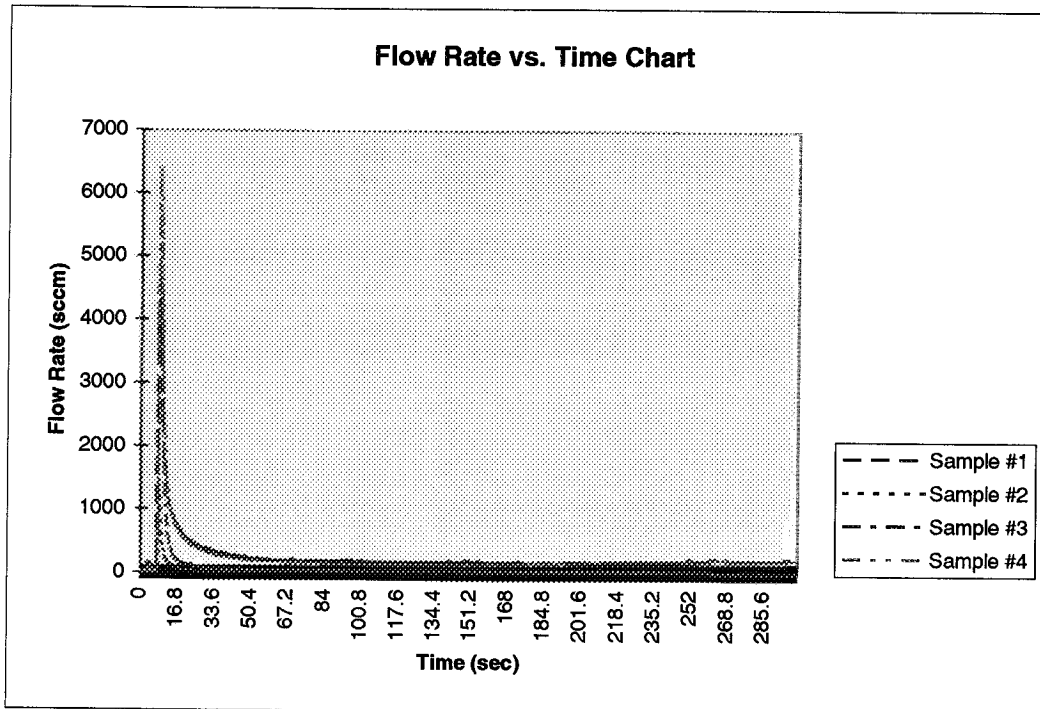
Sample Run	Max. Load (N)	Min. Pressure after Puncture (Pa)	Max. Flow Rate (sccm)	Min. Flow Rate after Puncture (sccm)	Delta Flow Rate Max. (-) Min. (sccm)	Delta Flow Rate Min. (-) Initial (sccm)	Change of Time from Max. to Min. Flow Rate (sec)	Volume Lost in 180 sec. After Max. Flow Rate (cm <sup>3</sup> )
1	33.86	28813.2	498.65	23.00	475.65	-0.08	30.00	81.31
2	28.35	29351.0	36.68	23.50	13.18	2.50	16.00	70.11
3	29.73	29426.8	275.00	146.88	128.12	127.60	386.00	692.93
4	34.59	29461.3	22.46	21.00	1.46	0.98	8.00	64.64
Cum. Avg	31.63	29263.1	208.20	53.60	154.60	32.75	110.00	227.25
Cum. Std Dev	2.59	224.94	178.63	46.64	160.52	47.42	138.00	232.84



**Laboratory Analysis Report  
Self-Sealing Performance Test**

Test Method	1275-70001	Sample Run	Weight of Sample Specimen (gm)	Average Initial Pressure (Pa)	Average Initial Flow Rate (sccm)
Log No.	8021-01	1	22.39	29531.9	26.82
Work Order No.	1275-17039	2	23.37	29542.4	23.42
Material	Tyrylner Urethane 30 mil	3	21.89	29510.8	27.48
Probe Used	Puncture Probe	4	23.46	29534.2	23.58
Thickness (cm)	0.0860 Dev 0.0011	Cum. Avg	22.78	29529.8	25.32
Weight	See Table	Cum. Std Dev	0.64	9.52	1.83
Date	May 14, 1998				

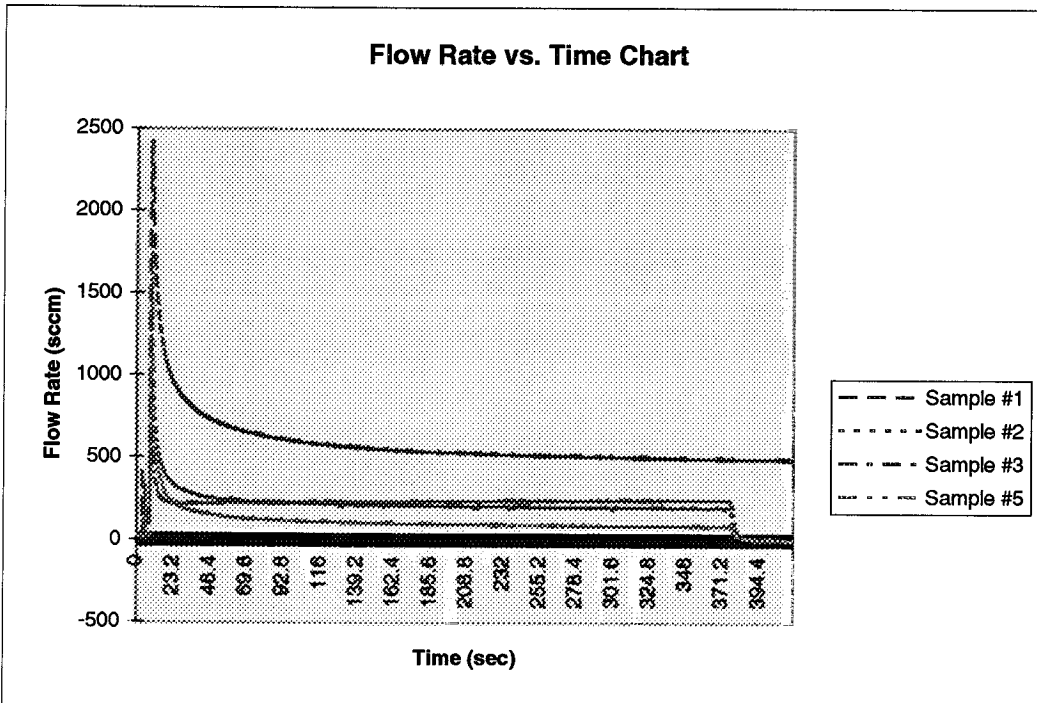
Sample Run	Max. Load (N)	Min. Pressure after Puncture (Pa)	Max. Flow Rate (sccm)	Min. Flow Rate after Puncture (sccm)	Delta Flow Rate Max. (-) Min. (sccm)	Delta Flow Rate Min. (-) Initial (sccm)	Change of Time from Max. to Min. Flow Rate (sec)	Volume Lost in 180 sec After Max Flow Rate (cm <sup>3</sup> )
1	50.67	28468.5	4329	122	4206.63	95.18	350.00	863.75
2	42.47	28696.0	1181	24	1157.12	0.58	30.00	110.63
3	60.34	27985.8	6190	49	6140.84	21.52	122.00	373.58
4	53.92	27958.2	6393	143	6250.09	119.42	113.00	820.86
Cum. Avg	51.85	28277.1	4523	85	4438.67	59.18	153.75	542.20
Cum. Std Dev	5.28	305.09	1768.3	48	1756.80	48.12	98.125	300.10



**Laboratory Analysis Report  
Self-Sealing Performance Test**

Test Method	1275-70001	Sample Run	Weight of Sample Specimen (gm)	Average Initial Pressure (Pa)	Average Initial Flow Rate (sccm)
Log No.	8021-01	1	21.4	29514.3	23.89
Work Order No.	1275-17039	2	21.8	29566.8	23.62
Material	Conathane EN-11, 30 mil	3	22.7	29528.2	23.06
Probe Used	Puncture Probe	5	21.9	29307.0	25.26
Thickness (cm)	0.0994 Dev 0.0017	Cum. Avg	21.9	29479.1	23.96
Weight	See Table	Cum. Std Dev	0.36	86.05	0.65
Date	May 14, 1998				

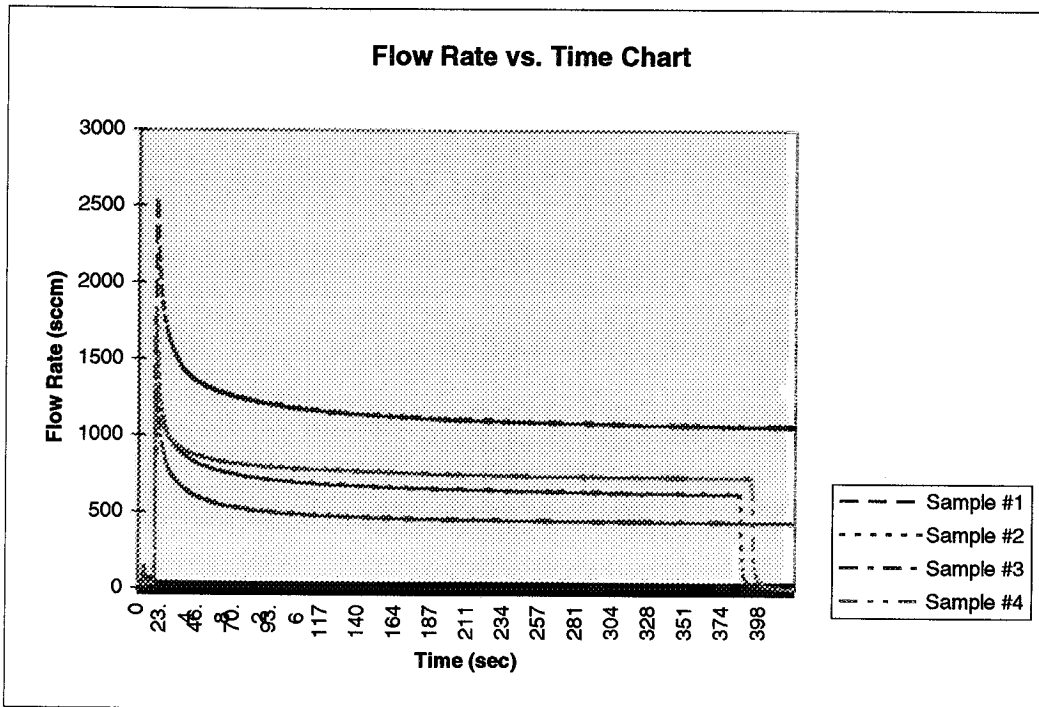
Sample Run	Max. Load (N)	Min. Pressure after Puncture (Pa)	Max. Flow Rate (sccm)	Min. Flow Rate after Puncture (sccm)	Delta Flow Rate Max. (-) Min. (sccm)	Delta Flow Rate Min. (-) Initial (sccm)	Change of Time from Max. to Min. Flow Rate (sec)	Volume Lost in 180 sec After Max. Flow Rate (cm <sup>3</sup> )
1	99.29	28613.2	2422	488.00	1933.78	464.11	356.00	2054.19
2	87.27	28613.2	1579	202.00	1377.19	178.38	210.00	773.32
3	85.37	28606.3	1162	220.00	942.48	196.94	11.00	711.49
5	67.77	28337.5	1743	86.00	1656.86	60.74	312.00	444.79
Cum. Avg	84.93	28542.6	1727	249	1477.58	225.04	222.25	995.95
Cum. Std Dev	8.58	102.56	356	120	317.74	119.53	111.75	529.12



**Laboratory Analysis Report  
Self-Sealing Performance Test**

Test Method	1275-70001	Sample Run		Weight of Sample Specimen (gm)		Average Initial Pressure (Pa)		Average Initial Flow Rate (sccm)	
Log No.	8021-01	1		6.16		30281.2		30.08	
Work Order No.	1275-17039	2		6.50		30289.7		22.37	
Material	Two Ply Blouse MG-01	3		6.17		29917.3		30.34	
Probe Used	Puncture Probe	4		6.32		29866.3		27.49	
Thickness	N/A	Cum. Avg		6.3		30088.6		27.57	
Weight	See Table	Cum. Std Dev		0.123		196.82		2.64	
Date	May 18, 1998								

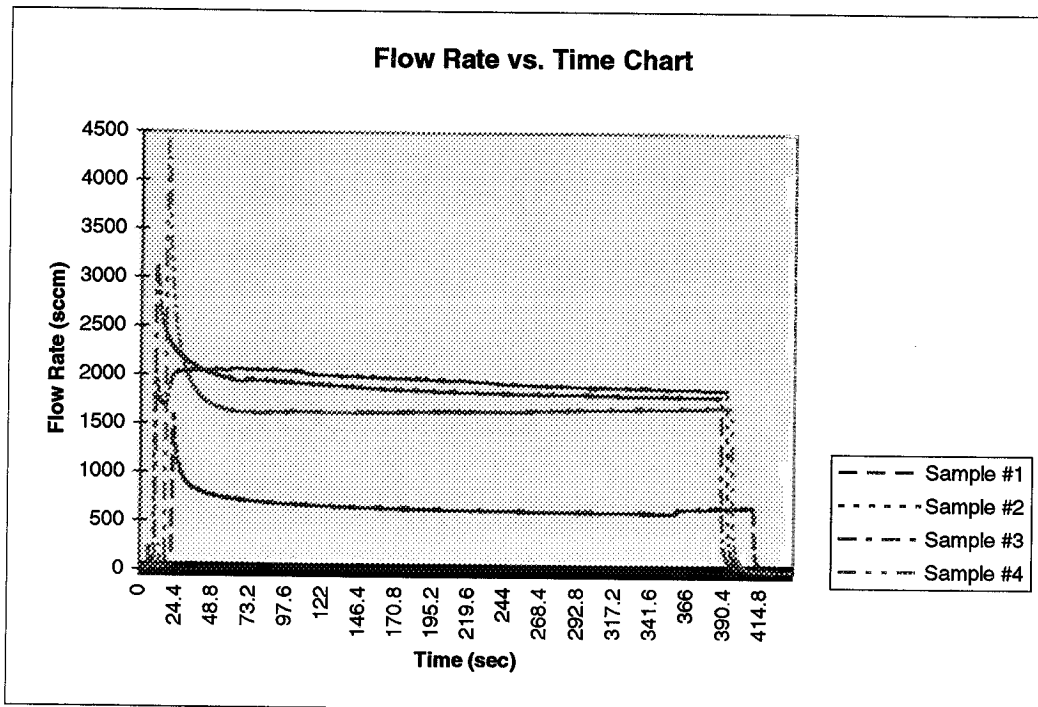
Sample Run	Max. Load (N)	Min. Pressure after Puncture (Pa)	Max. Flow Rate (sccm)	Min. Flow Rate after Puncture (sccm)	Delta Flow Rate Max. (-) Min. (sccm)	Delta Flow Rate Min. (-) Initial (sccm)	Change of Time from Max. to Min. Flow Rate (sec)	Volume Lost in 180 sec After Max Flow Rate (cm <sup>3</sup> )
1	60.26	29240.7	2545	1055	1490.00	1024.92	357.00	3749.59
2	48.99	29299.6	1667	622	1045.00	599.63	300.00	2231.20
3	45.55	29085.2	1439	430	1008.33	399.91	288.00	1596.57
4	50.73	27701.1	1810	726	1083.55	698.92	229.00	2462.23
Cum. Avg	51.38	28831.6	1865	708	1156.72	680.85	293.50	2509.90
Cum. Std Dev	4.44	565.25	340	182	166.64	181.07	35.00	619.85



**Laboratory Analysis Report  
Self-Sealing Performance Test**

Test Method	1275-70001	Sample Run	Weight of Sample Specimen (gm)	Average Initial Pressure (Pa)	Average Initial Flow Rate (sccm)
Log No.	8021-01	1	30.37	28798.3	31.66
Work Order No.	1275-17039	2	27.23	30239.3	23.34
Material	Silicone Vac Gre on Felt MG-02	3	23.36	29960.9	28.91
Probe Used	Puncture Probe	4	25.82	29845.9	24.13
Thickness	N/A	Cum. Avg	26.70	29711.1	27.01
Weight	See Table	Cum. Std Dev	2.11	456.41	3.28
Date	May 18, 1998				

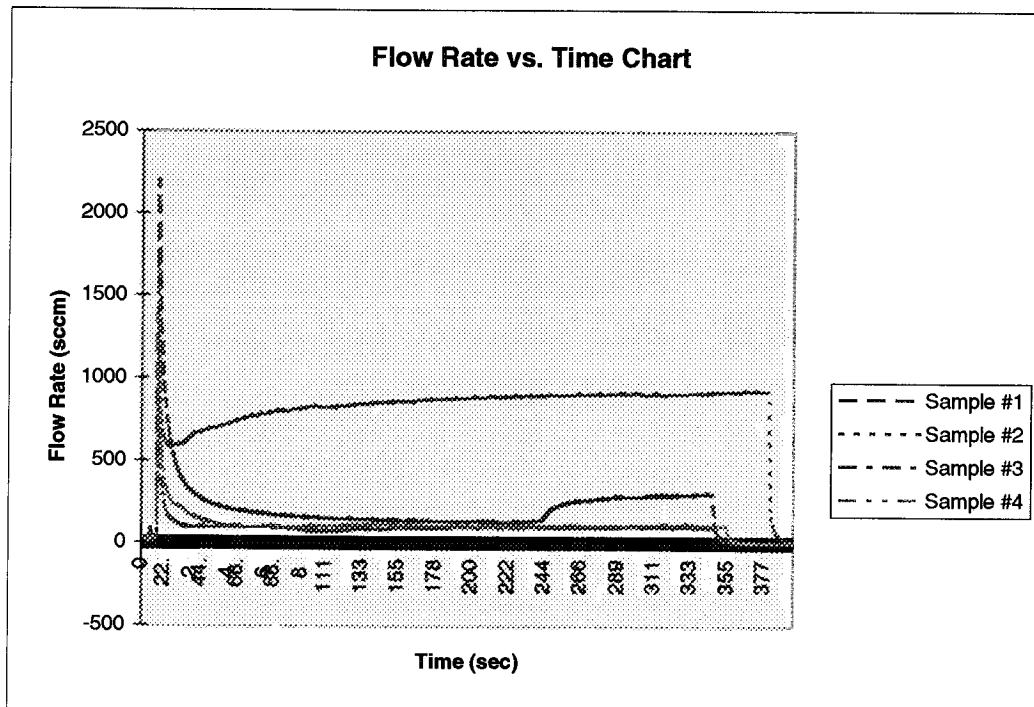
Sample Run	Max. Load (N)	Min. Pressure after Puncture (Pa)	Max. Flow Rate (sccm)	Min. Flow Rate after Puncture (sccm)	Delta Flow Rate Max. (-) Min. (sccm)	Delta Flow Rate Min. (-) Initial (sccm)	Change of Time from Max. Min. Flow Rate (sec)	Volume Lost in 180 sec After Max Flow Rate (cm <sup>3</sup> )
1	79.43	28744.1	1584	598	985.54	566.48	334.00	2120.12
2	57.08	28825.2	2062	1863	198.87	1839.79	378.40	6052.66
3	80.43	28932.1	3126	1787	1339.39	1758.05	347.40	5960.35
4	88.72	28787.7	4423	1617	2806.34	1592.86	109.00	5201.13
Cum. Avg	76.42	28822.3	2799	1466	1332.54	1439.29	292.20	4833.57
Cum. Std Dev	9.666	56.372	976	434	740.33	436.41	91.60	1356.72



**Laboratory Analysis Report  
Self-Sealing Performance Test**

Test Method	1275-70001	Sample Run	Weight of Sample Specimen (gm)	Average Initial Pressure (Pa)	Average Initial Flow Rate (sccm)
Log No.	8021-01	1	24.5	29920.1	26.24
Work Order No.	1275-17039	2	29.0	30113.7	20.28
Material	Tyrylner Isocynate on Felt MG-03	3	35.4	29975.6	29.04
Probe Used	Puncture Probe	4	32.5	29761.2	24.21
Thickness	N/A	Cum. Avg	30.3	29942.7	24.94
Weight	See Table	Cum. Std Dev	3.585	101.997	2.699
Date	May 18, 1998				

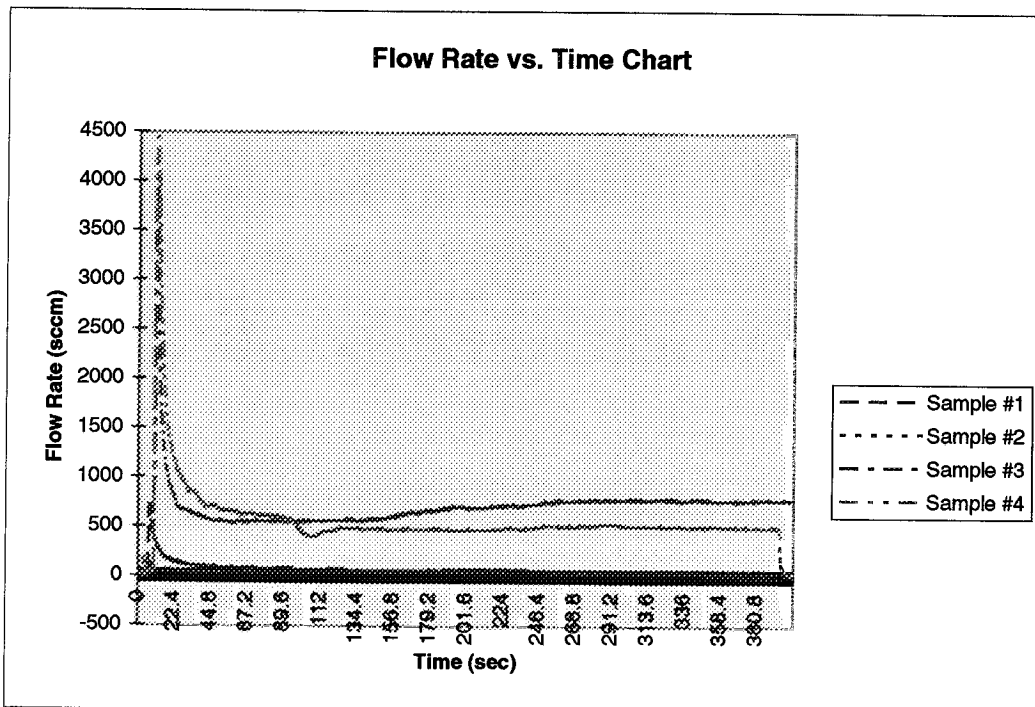
Sample Run	Max. Load (N)	Min. Pressure after Puncture (Pa)	Max. Flow Rate (sccm)	Min. Flow Rate after Puncture (sccm)	Delta Flow Rate Max. (-) Min. (sccm)	Delta Flow Rate Min. (-) Initial (sccm)	Change of Time from Max. Min. Flow Rate (sec)	Volume Lost in 180 sec. After Max. Flow Rate (cm <sup>3</sup> )
1	90.96	28906.8	2197	130	2067.43	103.33	212.20	677.25
2	88.60	29117.6	1350	581	768.79	560.84	8.00	2391.37
3	64.00	29302.0	1265	75	1189.64	46.32	98.60	315.66
4	65.84	29022.3	1662	82	1580.38	57.41	79.80	401.07
Cum. Avg	77.35	29087.2	1618	217	1401.56	191.98	99.65	946.34
Cum. Std Dev	12.431	122.622	311	182	422.35	184.43	56.28	722.52



**Laboratory Analysis Report  
Self-Sealing Performance Test**

Test Method	1275-70001	Sample Run	Weight of Sample Specimen (gm)	Average Initial Pressure (Pa)	Average Initial Flow Rate (sccm)
Log No.	8021-01	1	27.98	30313.4	27.00
Work Order No.	1275-17039	2	31.86	29938.9	19.74
Material	Conathane on Felt, MG-04	3	35.99	29983.9	29.27
Probe Used	Puncture Probe	4	36.25	29746.6	26.63
Thickness	N/A	Cum. Avg	33.02	29995.7	25.66
Weight (gm)	See Table	Cum. Std Dev	3.10	158.86	2.96
Date	May 26, 1998				

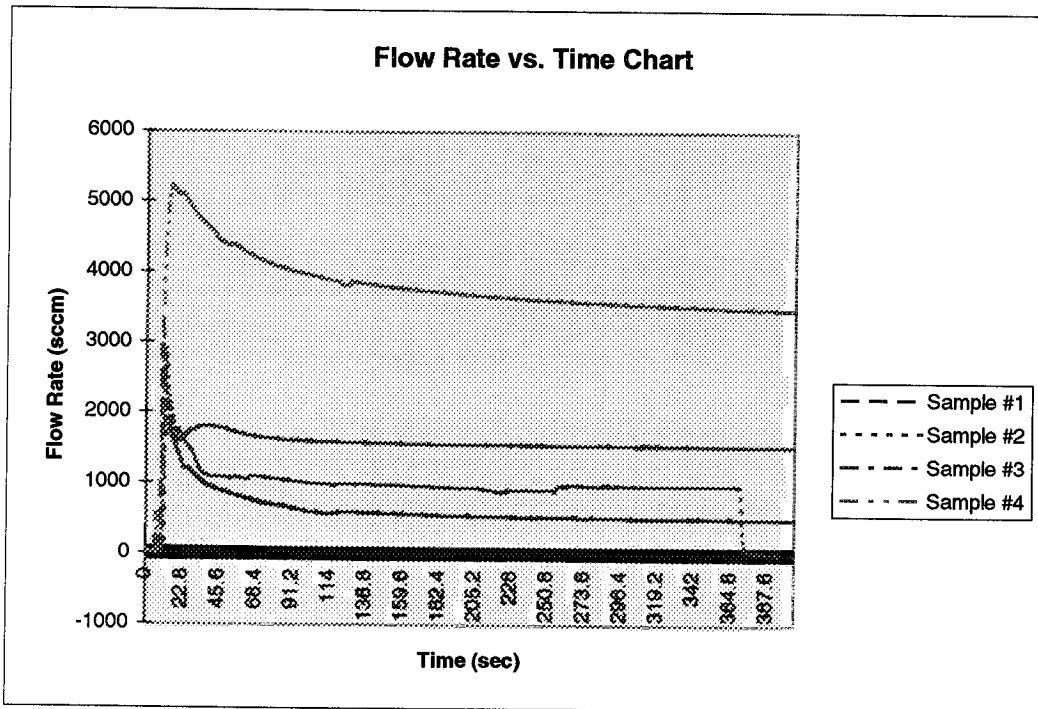
Sample Run	Max. Load (N)	Min. Pressure after Puncture (Pa)	Max. Flow Rate (sccm)	Min. Flow Rate after Puncture (sccm)	Delta Flow Rate Max. (-) Min. (sccm)	Delta Flow Rate Min. (-) Initial (sccm)	Change of Time from Max. to Min. Flow Rate (sec)	Volume Lost in 180 sec After Max Flow Rate (cm <sup>3</sup> )
1	135.27	29436.1	738	49	688.21	22.48	275.00	268.69
2	189.87	29492.3	129	33	95.55	13.63	143.00	126.89
3	78.26	28861.5	4225	539	3685.49	510.17	47.20	1970.85
4	79.69	28701.7	4481	396	4084.91	369.53	95.20	2024.51
Cum. Avg	120.77	29122.9	2393	255	2138.54	228.95	140.10	1097.73
Cum. Std Dev	41.800	341.308	1960	213	1746.66	210.90	68.90	899.95



**Laboratory Analysis Report  
Self-Sealing Performance Test**

Test Method	1275-70001	Sample Run		Weight of Sample Specimen (gm)		Average Initial Pressure (Pa)		Average Initial Flow Rate (sccm)	
Log No.	8021-01	1		30.05		30183.5		24.41	
Work Order No.	1275-17039	2		34.52		29783.8		23.26	
Material	Wacker Silgel on Felt, MG-05	3		36.88		29938.3		28.25	
Probe Used	Puncture Probe	4		30.12		29745.1		25.47	
Thickness	N/A	Cum. Avg		32.89		29912.7		25.35	
Weight (gm)	See Table	Cum. Std Dev		2.81		148.24		1.51	
Date	May 26, 1998								

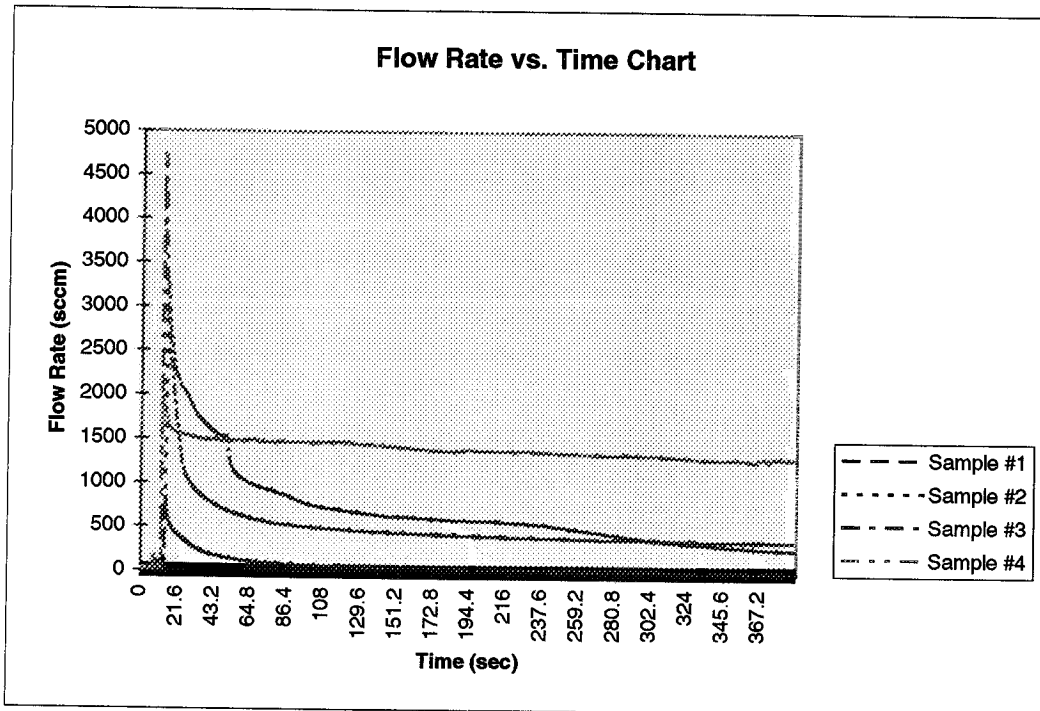
Sample Run	Max. Load (N)	Min. Pressure after Puncture (Pa)	Max. Flow Rate (sccm)	Min. Flow Rate after Puncture (sccm)	Delta Flow Rate Max. (-) Min. (sccm)	Delta Flow Rate Min. (-) Initial (sccm)	Change of Time from Max. to Min. Flow Rate (sec)	Volume Lost in 180 sec After Max Flow Rate (cm <sup>3</sup> )
1	88.04	29111.5	3314	499	2815.72	474.13	389.40	2332.94
2	91.14	28737.0	2910	879	2031.70	855.47	208.60	3308.25
3	73.90	29074.9	2430	1530	899.67	1502.01	480.00	4938.26
4	93.93	27475.5	5217	3461	1755.71	3435.73	406.60	12330.58
Cum. Avg	86.75	28599.7	3468	1592	1875.70	1566.83	371.15	5727.51
Cum. Std Dev	6.428	562.112	875	935	548.01	934.45	81.28	3301.54



**Laboratory Analysis Report  
Self-Sealing Performance Test**

Test Method	1275-70001	Sample Run	Weight of Sample Specimen (gm)	Average Initial Pressure (Pa)	Average Initial Flow Rate (sccm)
Log No.	8021-01	1	11.79	29239.6	30.92
Work Order No.	1275-17039	2	12.79	29239.5	29.10
Material	Sylgard Q3-6636, 15 mil	3	13.05	29594.4	26.09
Probe Used	Puncture Probe	4	12.74	29505.0	25.13
Thickness (cm)	0.0578 Dev 0.0019	Cum. Avg	12.59	29394.6	27.81
Weight	See Table	Cum. Std Dev	0.40	155.06	2.20
Date	June 24, 1998				

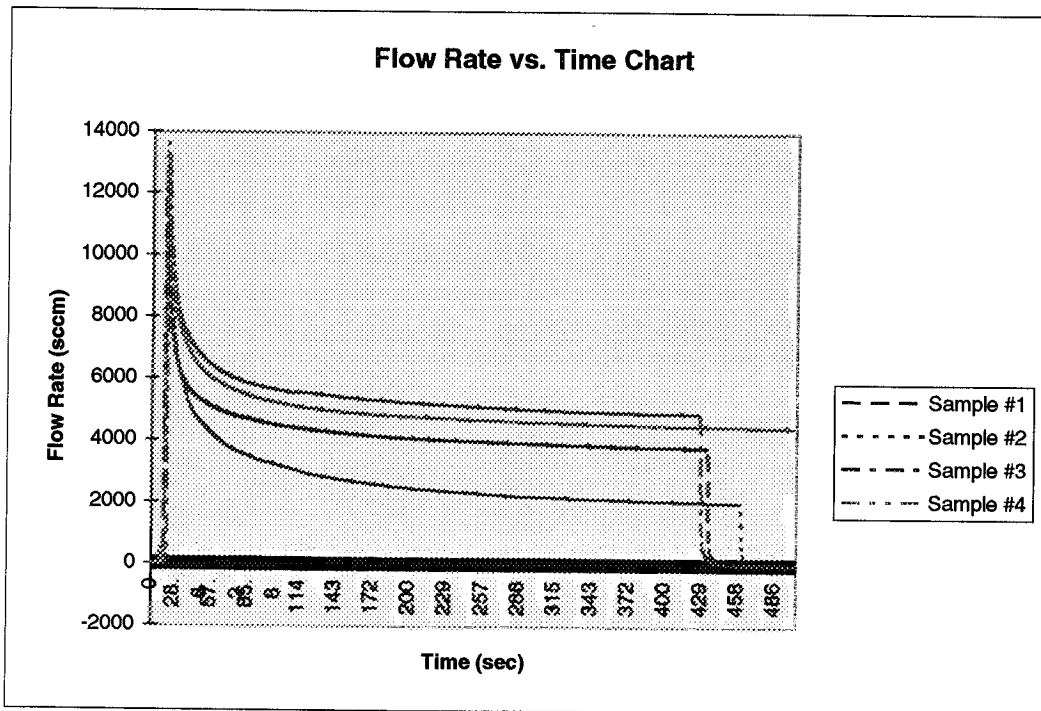
Sample Run	Max. Load (N)	Min. Pressure after Puncture (Pa)	Max. Flow Rate (sccm)	Min. Flow Rate after Puncture (sccm)	Delta Flow Rate Max. (-) Min. (sccm)	Delta Flow Rate Min. (-) Initial (sccm)	Change of Time from Max. to Min. Flow Rate (sec)	Volume Lost in 180 sec. After Max. Flow Rate (cm <sup>3</sup> )
1	38.50	28638.6	829	27	801.90	-4.28	233.40	339.581
2	48.66	28178.3	3258	185	3073.20	156.01	464.20	2936.49
3	54.34	28508.2	4716	352	4363.98	326.01	416.00	1991.51
4	48.94	28725.7	1996	1257	739.19	1231.68	351.80	4408.07
Cum. Avg	47.61	28512.7	2700	455	2244.57	427.35	366.35	2418.91
Cum. Std Dev	4.55	169.46	1287.5	400.82	1474.03	402.16	73.75	1253.37



**Laboratory Analysis Report  
Self-Sealing Performance Test**

Test Method	1275-70001	Sample Run	Weight of Sample Specimen (gm)	Average Initial Pressure (Pa)	Average Initial Flow Rate (sccm)
Log No.	8021-01	1	14.47	29443.7	25.08
Work Order No.	1275-17039	2	13.64	29443.8	26.15
Material	Tyrllyner Urethane 15 mil	3	14.52	29383.7	24.51
Probe Used	Puncture Probe	4	16.02	29353.3	25.63
Thickness (cm)	0.0708 Dev 0.0022	Cum. Avg	14.66	29406.1	25.34
Weight	See Table	Cum. Std Dev	0.68	37.64	0.55
Date	June 25, 1998				

Sample Run	Max. Load (N)	Min. Pressure after Puncture (Pa)	Max. Flow Rate (sccm)	Min. Flow Rate after Puncture (sccm)	Delta Flow Rate Max. (-) Min. (sccm)	Delta Flow Rate Min. (-) Initial (sccm)	Change of Time from Max. to Min. Flow Rate (sec)	Volume Lost in 180 sec After Max Flow Rate (cm <sup>3</sup> )
1	57.87	27594.7	12209	3794	8414	3769	423.0	14496
2	62.65	27444.8	13767	2010	11757	1983	440.4	10912
3	65.11	27403.4	13155	4887	8268	4863	414.2	18100
4	68.19	27299.8	13397	4418	8979	4392	525.6	16953
Cum. Avg	63.45	27435.7	13132	3777	9355	3752	450.8	15115
Cum. Std Dev	3.20	84.1	462	884	1201	884	37.4	2411





**APPENDIX C**  
**LABORATORY ANALYSIS REPORT, CUT PROTECTION PERFORMANCE TESTS**

# LABORATORY ANALYSIS REPORT

## CUT PROTECTION PERFORMANCE TEST

TRI/Environmental, Inc.  
9063 Bee Cave Road  
Austin, Texas 78733-6201

ILC Dover, Inc.  
One Moonwalker Road  
Frederica, Delaware 19946-2080

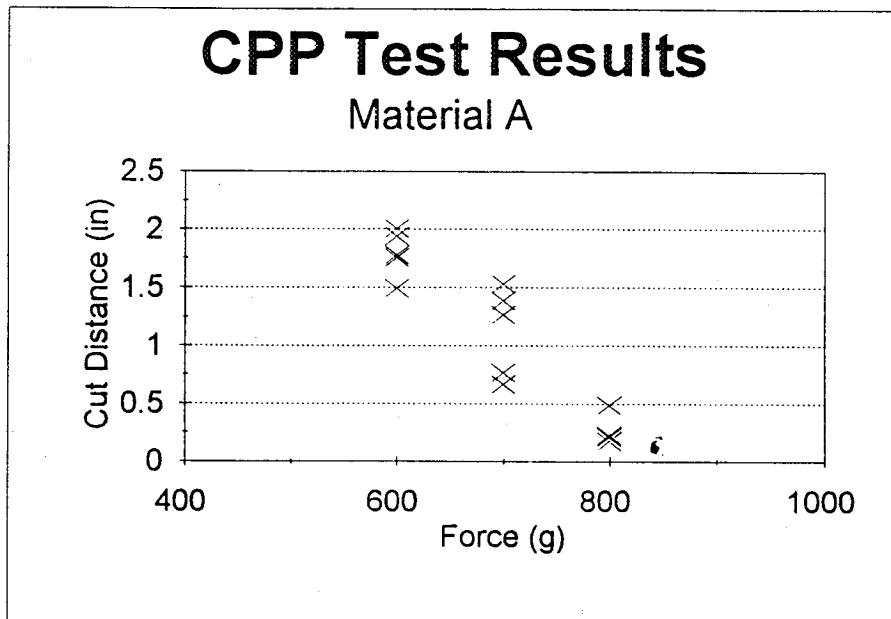
Instrumentation	Ashland CPP Cut Test Device
Standard	ASTM F1790
Job Number	98087
Log Number	98087-17-01
Material	Material A
Conditioning	None
Fabric Weight	7.1oz./square yard
Date	07/08/98

*[Signature]*  
Analyst

*[Signature]* 7/9/98  
QC

Interpolated Weight (g) to Cut after 1 inch of Blade Travel
674

Correlation Coefficient for Exponential Fit
R <sup>2</sup> = 0.831



Raw CPP Data

Client: ILC Dover  
 Job No.: 98087  
 Date: 07/08/98

Material: Material A  
 Log No.: 98087-17-01  
 Conditioning: None

Std Rubber Cut Distance(in (Calibration)	0.9945	0.9875	0.965	1.045	0.995	Calibration Average 0.9974
---	--------	--------	-------	-------	-------	----------------------------------

Force (g)	CutDist.(in)	Corrected CutDist.(in)	Log Cut Distance
600	1.773	1.778	0.25
600	1.752	1.757	0.24
600	2	2.005	0.30
600	1.9295	1.935	0.29
600	1.486	1.490	0.17
700	1.266	1.269	0.10
700	0.6635	0.665	-0.18
700	1.53	1.534	0.19
700	1.3815	1.385	0.14
700	0.7655	0.767	-0.11
800	0.4845	0.486	-0.31
800	0.175	0.175	-0.76
800	0.2155	0.216	-0.67
800	0.2125	0.213	-0.67
800	0.225	0.226	-0.65

Regression Output:

Constant	2.90608
Std Err of Y Est	0.17023
R Squared	0.83135
No. of Observations	15
Degrees of Freedom	13
X Coefficient(s)	-0.00431
Std Err of Coef.	0.00054

# LABORATORY ANALYSIS REPORT

## CUT PROTECTION PERFORMANCE TEST

TRI/Environmental, Inc.  
9063 Bee Cave Road  
Austin, Texas 78733-6201

Instrumentation	Ashland CPP Cut Test Device
Standard	ASTM F1790
Job Number	98087
Log Number	98087-17-02
Material	Material B
Conditioning	None
Fabric Weight	7.83oz./square yard
Date	07/08/98

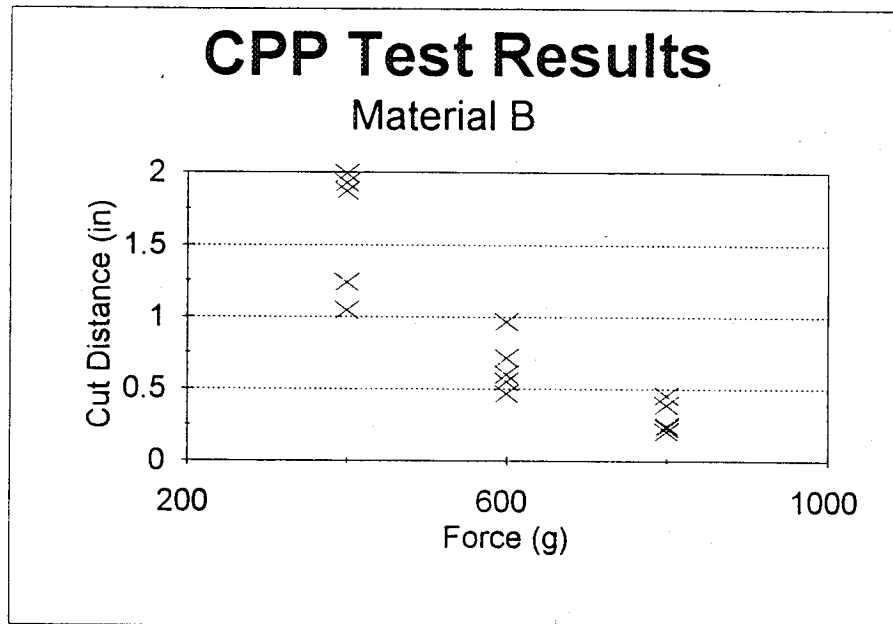
ILC Dover, Inc.  
One Moonwalker Road  
Frederica, Delaware 19946-2080

*[Signature]*  
Analyst

*[Signature]* 7/9/98  
QC

Interpolated Weight (g) to Cut after 1 inch of Blade Travel
502

Correlation Coefficient for Exponential Fit
R <sup>2</sup> = 0.860



Raw CPP Data

Client: ILC Dover  
 Job No.: 98087  
 Date: 07/08/98

Material: Material B  
 Log No.: 98087-17-02  
 Conditioning: None

Std Rubber Cut Distance(in (Calibration)	0.9945	0.9875	0.965	1.045	0.995	Calibration Average 0.9974
---	--------	--------	-------	-------	-------	----------------------------------

Force (g)	CutDist.(in)	Corrected CutDist.(in)	Log Cut Distance
400	1.926	1.931	0.29
400	1.865	1.870	0.27
400	1.9865	1.992	0.30
400	1.043	1.046	0.02
400	1.2345	1.238	0.09
600	0.5475	0.549	-0.26
600	0.4665	0.468	-0.33
600	0.7135	0.715	-0.15
600	0.598	0.600	-0.22
600	0.9605	0.963	-0.02
800	0.2305	0.231	-0.64
800	0.202	0.203	-0.69
800	0.244	0.245	-0.61
800	0.452	0.453	-0.34
800	0.3875	0.389	-0.41

Regression Output:	
Constant	0.91923
Std Err of Y Est	0.12972
R Squared	0.8599
No. of Observations	15
Degrees of Freedom	13
X Coefficient(s)	-0.00183
Std Err of Coef.	0.00021

# LABORATORY ANALYSIS REPORT

## CUT PROTECTION PERFORMANCE TEST

TRI/Environmental, Inc.  
9063 Bee Cave Road  
Austin, Texas 78733-6201

Instrumentation	Ashland CPP Cut Test Device
Standard	ASTM F1790
Job Number	98087
Log Number	98087-17-03
Material	Material C
Conditioning	None
Fabric Weight	11.51oz./square yard
Date	07/08/98

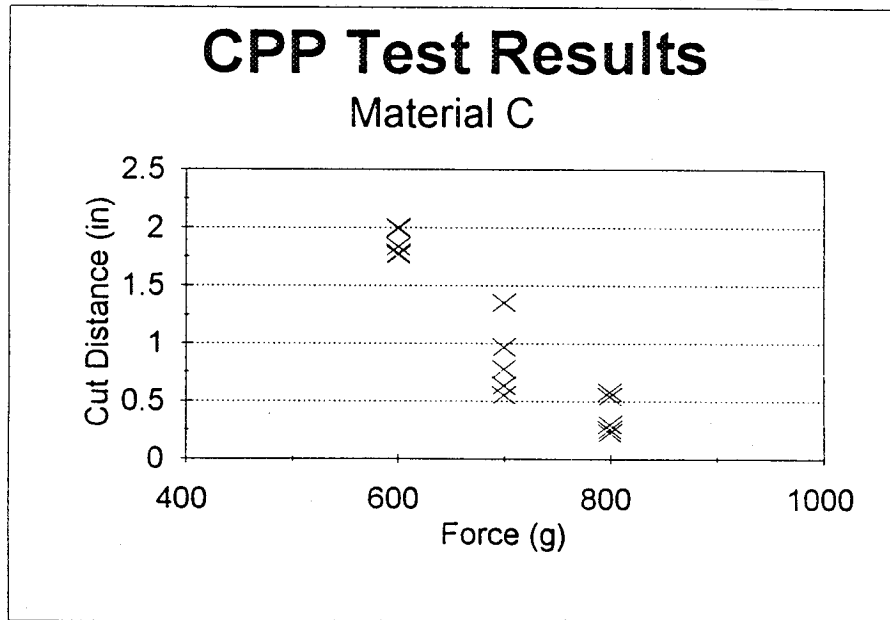
ILC Dover, Inc.  
One Moonwalker Road  
Frederica, Delaware 19946-2080

*[Signature]*  
Analyst

*[Signature]* 7/9/98  
QC

Interpolated Weight (g) to Cut after 1 inch of Blade Travel
675

Correlation Coefficient for Exponential Fit
R <sup>2</sup> = 0.846



Raw CPP Data

Client: ILC Dover  
 Job No.: 98087  
 Date: 07/08/98

Material: Material C  
 Log No.: 98087-17-03  
 Conditioning: None

Std Rubber Cut Distance(in (Calibration)	0.9945	0.9875	0.965	1.045	0.995	Calibration Average 0.9974
---	--------	--------	-------	-------	-------	----------------------------------

Force (g)	CutDist.(in)	Corrected CutDist.(in)	Log Cut Distance
600	1.9855	1.991	0.30
600	2	2.005	0.30
600	1.762	1.767	0.25
600	1.832	1.837	0.26
600	1.7755	1.780	0.25
700	0.6315	0.633	-0.20
700	0.777	0.779	-0.11
700	1.35	1.354	0.13
700	0.551	0.552	-0.26
700	0.9635	0.966	-0.02
800	0.54	0.541	-0.27
800	0.58	0.582	-0.24
800	0.255	0.256	-0.59
800	0.2285	0.229	-0.64
800	0.2985	0.299	-0.52

Regression Output:

Constant	2.4451
Std Err of Y Est	0.13565
R Squared	0.8457
No. of Observations	15
Degrees of Freedom	13
X Coefficient(s)	-0.00362
Std Err of Coef.	0.00043

# LABORATORY ANALYSIS REPORT

## CUT PROTECTION PERFORMANCE TEST

TRI/Environmental, Inc.  
9063 Bee Cave Road  
Austin, Texas 78733-6201

Instrumentation Standard	Ashland CPP Cut Test Device ASTM F1790
Job Number	98087
Log Number	98087-17-04
Material	Material D
Conditioning	None
Fabric Weight	15.69oz./square yard
Date	07/08/98

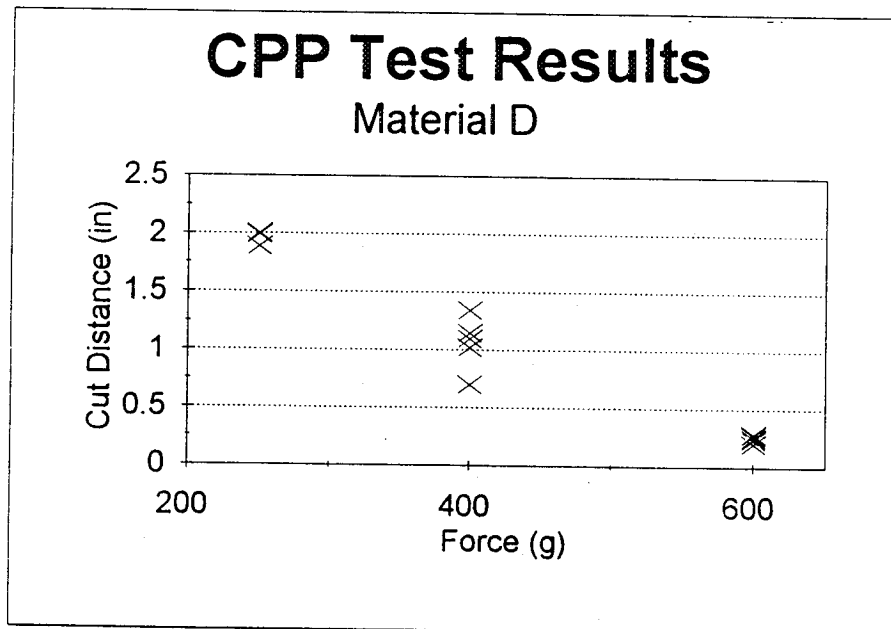
ILC Dover, Inc.  
One Moonwalker Road  
Frederica, Delaware 19946-2080

*Clifford*  
Analyst

*John 7/9/98*  
QC

Interpolated Weight (g) to Cut after 1 inch of Blade Travel
379

Correlation Coefficient for Exponential Fit
R <sup>2</sup> = 0.956



Raw CPP Data

Client: ILC Dover  
 Job No.: 98087  
 Date: 07/08/98

Material: Material D  
 Log No.: 98087-17-04  
 Conditioning: None

Std Rubber Cut Distance(in (Calibration)	0.9945	0.9875	0.965	1.045	0.995	Calibration Average 0.9974
---	--------	--------	-------	-------	-------	----------------------------------

Force (g)	CutDist.(in)	Corrected CutDist.(in)	Log Cut Distance	Regression Output:	
				Constant	0.99109
250	1.9865	1.992	0.30	Std Err of Y Est	0.08608
250	2	2.005	0.30	R Squared	0.95634
250	1.885	1.890	0.28	No. of Observations	15
250	2	2.005	0.30	Degrees of Freedom	13
250	1.9965	2.002	0.30		
400	0.699	0.701	-0.15	X Coefficient(s)	-0.00262
400	1.0945	1.097	0.04	Std Err of Coef.	0.00016
400	1.1415	1.144	0.06		
400	1.0145	1.017	0.01		
400	1.34	1.343	0.13		
600	0.2715	0.272	-0.57		
600	0.248	0.249	-0.60		
600	0.2015	0.202	-0.69		
600	0.281	0.282	-0.55		
600	0.233	0.234	-0.63		

**APPENDIX D**  
**LABORATORY ANALYSIS REPORT, PUNCTURE RESISTANCE TESTS**

# LABORATORY ANALYSIS REPORT

## PUNCTURE RESISTANCE TEST

TRI/Environmental, Inc.  
9063 Bee Cave Rd.  
Austin, TX 78733

ILC Dover  
One Moonwalker Rd.  
Frederica, DE 19946-2080

METHOD NO.	ASTM F1342
LOG NO.	98087-17-01
DATE	07/09/98
MATERIAL	Material A

*Janett A Nelson*  
ANALYST

*J. Nelson 7/10/98*  
QC

SWATCH NUMBER	PUNCTURE NUMBER	LOAD (lb)
A1	1	1.0
	2	0.9
	3	2.4
A2	1	0.4
	2	1.4
	3	1.6
A3	1	2.0
	2	0.8
	3	0.7
A4	1	2.5
	2	0.8
	3	1.3
CUM. AVG		1.3
CUM. STD DEV		0.7

# LABORATORY ANALYSIS REPORT

## PUNCTURE RESISTANCE TEST

TRI/Environmental, Inc.  
9063 Bee Cave Rd.  
Austin, TX 78733

ILC Dover  
One Moonwalker Rd.  
Frederica, DE 19946-2080

METHOD NO.	ASTM F1342
LOG NO.	98087-17-02
DATE	07/09/98
MATERIAL	Material B

*Janett A. Nole*

ANALYST

*John 7/10/98*  
QC

SWATCH NUMBER	PUNCTURE NUMBER	LOAD (lb)
B1	1	1.2
	2	1.3
	3	0.5
B2	1	1.0
	2	0.9
	3	3.3
B3	1	0.8
	2	2.4
	3	1.7
B4	1	1.5
	2	1.4
	3	4.7
CUM. AVG		1.7
CUM. STD DEV		1.2

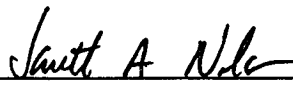
# LABORATORY ANALYSIS REPORT

## PUNCTURE RESISTANCE TEST

TRI/Environmental, Inc.  
9063 Bee Cave Rd.  
Austin, TX 78733

ILC Dover  
One Moonwalker Rd.  
Frederica, DE 19946-2080

METHOD NO.	ASTM F1342
LOG NO.	98087-17-03
DATE	07/09/98
MATERIAL	Material C

  
ANALYST

  
QC

SWATCH NUMBER	PUNCTURE NUMBER	LOAD (lb)
C1	1	0.3
	2	0.8
	3	0.8
C2	1	2.0
	2	0.7
	3	0.7
C3	1	0.8
	2	2.3
	3	0.7
C4	1	1.1
	2	1.1
	3	2.3
CUM. AVG		1.1
CUM. STD DEV		0.6

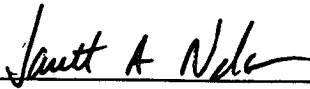
# LABORATORY ANALYSIS REPORT

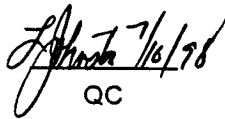
## PUNCTURE RESISTANCE TEST

TRI/Environmental, Inc.  
9063 Bee Cave Rd.  
Austin, TX 78733

ILC Dover  
One Moonwalker Rd.  
Frederica, DE 19946-2080

METHOD NO.	ASTM F1342
LOG NO.	98087-17-04
DATE	07/09/98
MATERIAL	Material D

  
ANALYST

  
QC

SWATCH NUMBER	PUNCTURE NUMBER	LOAD (lb)
D1	1	3.1
	2	1.8
	3	3.1
D2	1	2.5
	2	2.9
	3	1.7
D3	1	2.9
	2	2.9
	3	3.5
D4	1	4.0
	2	2.6
	3	3.0
CUM. AVG		2.8
CUM. STD DEV		0.6

**APPENDIX E**  
**HYPERVELOCITY IMPACT RESISTANCE TEST REPORTS**

**Summary of Preliminary  
Hypervelocity Impact Testing Results**

	Hypervelocity Test #1 Prototype A	Hypervelocity Test #2 Prototype B	Hypervelocity Test #3 Prototype C	Hypervelocity Test #4 Incumbent Fabric	Hypervelocity Test #5 Prototype A	Hypervelocity Test #6 Prototype B
<b>Velocity (km/s)</b>	7.2	7.0	7.1	7.0	7.1	7.07
<b>Projectile Diameter (mm)</b>	0.5	0.5	0.5	0.5	0.6	0.6
<b>Angle (degree)</b>	0	0	0	0	0	0
<b>Prototype Layer</b>	1.0 mm diameter hole	1.0 mm diameter hole	1.75 mm X 1.5 mm diameter hole	0.75 mm X 1 mm diameter hole	1.5 mm X 1.25 mm diameter hole	1 mm hole
<b>Reinforced Mylar Layer #1</b>	2.5 mm X 2.5 mm entrance hole	3.75 mm X 3.0 mm entrance hole	4.0 mm X 3.25 mm entrance hole	3.0 mm X 4.0 mm entrance hole	3.75 mm X 2.5 mm entrance hole	2.75 mm X 2.75 mm hole w/ petals
<b>Reinforced Mylar Layer #5</b>	5.0 mm X 5.0 mm exit hole	4.75 mm X 5.5 mm exit hole	5.0 mm X 5.5 mm exit hole	5.0 mm X 5.0 mm exit hole	5.0 mm X 5.0 mm exit hole	7.0 mm X 6.0 mm exit hole
<b>Neoprene Coated Nylon</b>	1.0 mm X 1.5 mm hole	1.25 mm X 1.75 mm hole	1.0 mm X 1.25 mm hole	1.25 mm X 2.25 mm hole	2.25 mm X 2.0 mm hole	2.0 mm X 2.25 mm hole
<b>Dacron Polyester</b>	2.25 mm X 3.25 mm hole	2.0 mm X 3.0 mm hole	1.5 mm X 1.25 mm hole	2.5 mm X 1.75 mm hole	3.25 mm X 4.0 mm hole	3.0 mm X 3.0 mm hole
<b>Urethane Coated Nylon</b>	4.5 mm X 6.5 mm Stain	.75 mm X 1.25 mm Hole 4.5 mm X 5.0 mm Stain	0.75 mm hole	.75 X 1.25 mm hole 3 mm X 3.5 mm Stain	0.5 mm Hole 5.0 mm Stain	1.5 mm Hole 5.0 X 6.0 mm Stain
<b>Aluminum Witness Plate</b>	No Damage Occurred	32 mm X 19 mm Splattered Area	0.25 mm craters 35 mm X 20 mm Splattered Area	32 mm X 30 mm Splattered Area	No Damage Detected	Minute Craters 45 mm X 30 mm Area
<b>Pass/Fail</b>	Passed	Failed	Failed	Failed	Failed	Failed

### Summary of Preliminary Hypervelocity Impact Testing Results

	Hypervelocity Test #7 Prototype C	Hypervelocity Test #9 Prototype A	Hypervelocity Test #10 Prototype A	Hypervelocity Test #11 Prototype B	Hypervelocity Test #12 Incumbent Fabric	Hypervelocity Test #13 Prototype C
<b>Velocity (km/s)</b>	7.17	7.0	7.0	7.1	6.9	7.0
<b>Projectile Diameter (mm)</b>	0.6	0.5	0.4	0.4	0.4	0.4
<b>Angle (degree)</b>	0	0	0	0	0	0
<b>Prototype Layer</b>	1.25 mm X 1.5 mm vertical hole	1.25 mm hole	0.75 mm hole	0.75 mm X 1 mm hole	1 mm hole	1 mm X 0.75 mm hole
<b>Reinforced Mylar Layer #1</b>	3.75 mm X 3.25 mm entrance w/ petals	3.5 mm X 5.0 mm entrance w/petals	2 mm X 1.5 mm entrance w/petals	1.75 mm X 1.75 mm entrance w/petals	2.0 mm entrance hole w/ petals	4.0 mm X 2.5 mm entrance hole w/ petals
<b>Reinforced Mylar Layer #5</b>	7.5 mm X 4.5 mm exit hole	4.5 mm X 5 mm exit hole	3.9 mm X 3.0 mm exit hole	4.5 mm X 4.0 mm exit hole	4.25 mm X 4.0 mm exit hole	2.75 mm X 2.0 mm exit hole
<b>Neoprene Coated Nylon</b>	2.5 mm X 2.25 mm hole	1.75 mm X 1.25 mm hole	1.25 mm hole	1 mm X 1 mm hole	0.75 mm X 0.5 mm hole	1.0 mm X 1.0 mm hole
<b>Dacron Polyester</b>	2.5 mm X 2.5 mm hole	2.5 mm X 1.25 mm hole	1.5 mm X 1.75 mm hole	1.25 mm X 1.5 mm hole	<0.25 mm X 0.5 mm hole	1.0 mm X 0.75 mm hole
<b>Urethane Coated Nylon</b>	1 mm X 0.75 mm Hole 5.0 mm X 4.5 mm Stain	1.25 mm X 0.75 mm hole 4.0 mm X 2.75 mm Stain	0.75 mm Hole 3 mm Stain	1.0 mm area of Broken Fibers 2.5 mm X 2.0 mm Stain	1.5 mm X 2.5 mm Stain	0.75 mm X 1.0 mm hole 2.0 mm X 2.5 mm Stain
<b>Aluminum Witness Plate</b>	Minute Craters 40 mm X 45 mm	Minute Craters 40 mm X 35 mm	Minute Craters 30 mm X 30 mm	Minute Craters 27 mm X 35 mm	No Damage Noted	No Damage Noted
<b>Pass/Fail</b>	Failed	Failed	Failed	Failed	Passed	Failed

NOTE: Hypervelocity Test #8 is not indicated, as it was reported as "a bad shot".

# REPORT DOCUMENTATION PAGE

Form Approved  
OMB No. 0704-0188

Public reporting burden for this collection of information is estimated to average 1 hour per response, including the time for reviewing instructions, searching existing data sources, gathering and maintaining the data needed, and completing and reviewing the collection of information. Send comments regarding this burden estimate or any other aspect of this collection of information, including suggestions for reducing this burden, to Washington Headquarters Services, Directorate for Information Operations and Reports, 1215 Jefferson Davis Highway, Suite 1204, Arlington, VA 22202-4302, and to the Office of Management and Budget, Paperwork Reduction Project (0704-0188), Washington, DC 20503.

<b>1. AGENCY USE ONLY (Leave Blank)</b>	<b>2. REPORT DATE</b> September 25, 1998	<b>3. REPORT TYPE AND DATES COVERED</b> Final Report 17 Sept 97 - 30 Sept 98
---	---	---

<b>4. TITLE AND SUBTITLE</b> NASA Research Announcement Final Report For Space Suit Survivability Enhancement	<b>5. FUNDING NUMBERS</b>  Contract: NASW-97014
--	--

<b>6. AUTHOR(S)</b> Thad H. Frderickson Joanne S. Ware	 John K. Lin Christopher M. Pastore
--	---

<b>7. PERFORMING ORGANIZATION NAME(S) AND ADDRESS(ES)</b> ILC Dover, Inc. Philadelphia College of Textiles One Moonwalker Rd. and Science Frederica, DE 19946 School House Lane & Henry Avenue Philadelphia, PA 199144-5497	<b>8. PERFORMING ORGANIZATION REPORT NUMBER</b>  1275
---	---

<b>9. SPONSORING / MONITORING AGENCY NAME(S) AND ADDRESS(ES)</b> NASA/Goddard Space Flight Center Greenbelt Rd. Greenbelt, MD 20221	<b>10. SPONSORING / MONITORING AGENCY REPORT NUMBER</b>  N/A
--	--

<b>11. SUPPLEMENTARY NOTES</b> N/A
---------------------------------------

<b>12a. DISTRIBUTION / AVAILABILITY STATEMENT</b> Available to public via NASA Center For Aerospace Information 800 Elkridge Landing Rd. Linthicum Heights, MD 21090-6934	<b>12b. DISTRIBUTION CODE</b>
---	-------------------------------

<b>13. ABSTRACT (Maximum 200 words)</b>  This report documents the research activities for space suit survivability material enhancements. Self-sealing mechanisms for the pressure envelope were addressed, as were improvements in materials for cut, puncture, and hypervelocity impact resistance.
--

<b>14. SUBJECT TERMS</b> Space Suit, Survivability, Self-Sealing, Cut Resistance, Puncture Resistance, Hypervelocity Impact Resistance, Cut Resistance Testing, Puncture Resistance Testing, Hypervelocity Impact Resistance Testing	<b>15. NUMBER OF PAGES</b> 78
<b>16. PRICE CODE</b>	

<b>17. SECURITY CLASSIFICATION OF REPORT</b> Unclassified	<b>18. SECURITY CLASSIFICATION OF THIS PAGE</b> Unclassified	<b>19. SECURITY CLASSIFICATION OF ABSTRACT</b> Unclassified	<b>20. LIMITATION OF ABSTRACT</b> SAR
--	---	--	--

NSN 7540-01-280-5500

Standard Form 298 (Rev. 2-89)  
Prescribed by ANSI Std. Z39-18  
298-102